Developmental Cognitive Neuroscience 52 (2021) 101032

Contents lists available at ScienceDirect

Developmental Cognitive Neuroscience

journal homepage: www.elsevier.com/locate/dcn

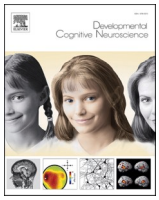

Pubertal timing and functional neurodevelopmental alterations independently mediate the effect of family conflict on adolescent psychopathology

Raluca Petrican [*], Sian Miles [1], Lily Rudd [1], Wiktoria Wasiewska [1], Kim S. Graham, Andrew D. Lawrence

Cardiff University Brain Research Imaging Centre (CUBRIC), School of Psychology, Cardiff University, Maindy Road, Cardiff CF24 4HQ, United Kingdom

ARTICLE INFO

Keywords:
Neurodevelopment
Early life adversity
BOLD variability
Structure-function coupling
Functional brain networks
Externalizing problems
Transcriptomics

ABSTRACT

This study tested the hypothesis that early life adversity (ELA) heightens psychopathology risk by concurrently altering pubertal and neurodevelopmental timing, and associated gene transcription signatures. Analyses focused on threat- (family conflict/neighbourhood crime) and deprivation-related ELAs (parental inattentiveness/unmet material needs), using longitudinal data from 1514 biologically unrelated youths in the Adolescent Brain and Cognitive Development (ABCD) study. Typical developmental changes in white matter microstructure corresponded to widespread BOLD signal variability ($BOLD_{sv}$) increases (linked to cell communication and biosynthesis genes) and region-specific task-related $BOLD_{sv}$ increases/decreases (linked to signal transduction, immune and external environmental response genes). Increasing resting-state (RS), but decreasing task-related $BOLD_{sv}$ predicted normative functional network segregation. Family conflict was the strongest concurrent and prospective contributor to psychopathology, while material deprivation constituted an additive risk factor. ELA-linked psychopathology was predicted by higher Time 1 threat-evoked $BOLD_{SV}$ (associated with axonal development, myelination, cell differentiation and signal transduction genes), reduced Time 2 RS $BOLD_{sv}$ (associated with cell metabolism and attention genes) and greater Time 1 to Time 2 control/attention network segregation. Earlier pubertal timing and neurodevelopmental alterations independently mediated ELA effects on psychopathology. Our results underscore the differential roles of the immediate and wider external environment(s) in concurrent and longer-term ELA consequences.

Early life adversity (ELA) is a robust predictor of long-term sequelae across species (Peverill et al., 2021; Selous et al., 2020; Snyder-Mackler et al., 2020). Nonetheless, the observed developmental alterations can vary widely as a function of the timing and type of adversity, which renders their characterisation a priority for designing more sensitive detection instruments and personalised interventions (Graham et al., 2021; McLaughlin et al., 2020; Murthy and Gould, 2020; Nelson and Gabard-Durnam, 2020).

To this end, here, we adopt a multilevel approach spanning behaviour, subjective experience, brain structure/function and gene expression in order to elucidate developmental mechanisms through which different ELAs heighten vulnerability to psychopathology in adolescence, a period typified by increased neural plasticity, and, thus, liability to environmental influences (Lopez et al., 2021; Worthman and Trang, 2018; Worthman and Trang, 2018). Our focus was on threat, conceptualised as actual or potential harm to the youth through exposure to violence, and deprivation, conceived as absence of expected environmental support (e.g., resources and/or cognitive, social, emotional stimulation) (McLaughlin et al., 2019). These two ELAs reportedly heighten psychopathology risk by accelerating biological aging (e.g., earlier pubertal onset, primarily for threat) and speeding structural development, thereby likely precluding fine tuning, of complementary neurocognitive pathways relevant to environmental salience (threat) versus cognitive control, memory and visual processing (deprivation) (for a meta-analysis, see Colich et al., 2020a, 2020b).

Capitalizing on these ELA type-specific neurostructural effects (but see Gehred et al., 2021), we examined the differential impact of threat versus deprivation on whole-brain functional maturation for which a

* Corresponding author.
E-mail address: petricanr@cardiff.ac.uk (R. Petrican).
[1] These authors contributed equally to this work and they are listed alphabetically based on their surnames.

https://doi.org/10.1016/j.dcn.2021.101032
Received 27 May 2021; Received in revised form 29 October 2021; Accepted 4 November 2021
Available online 6 November 2021

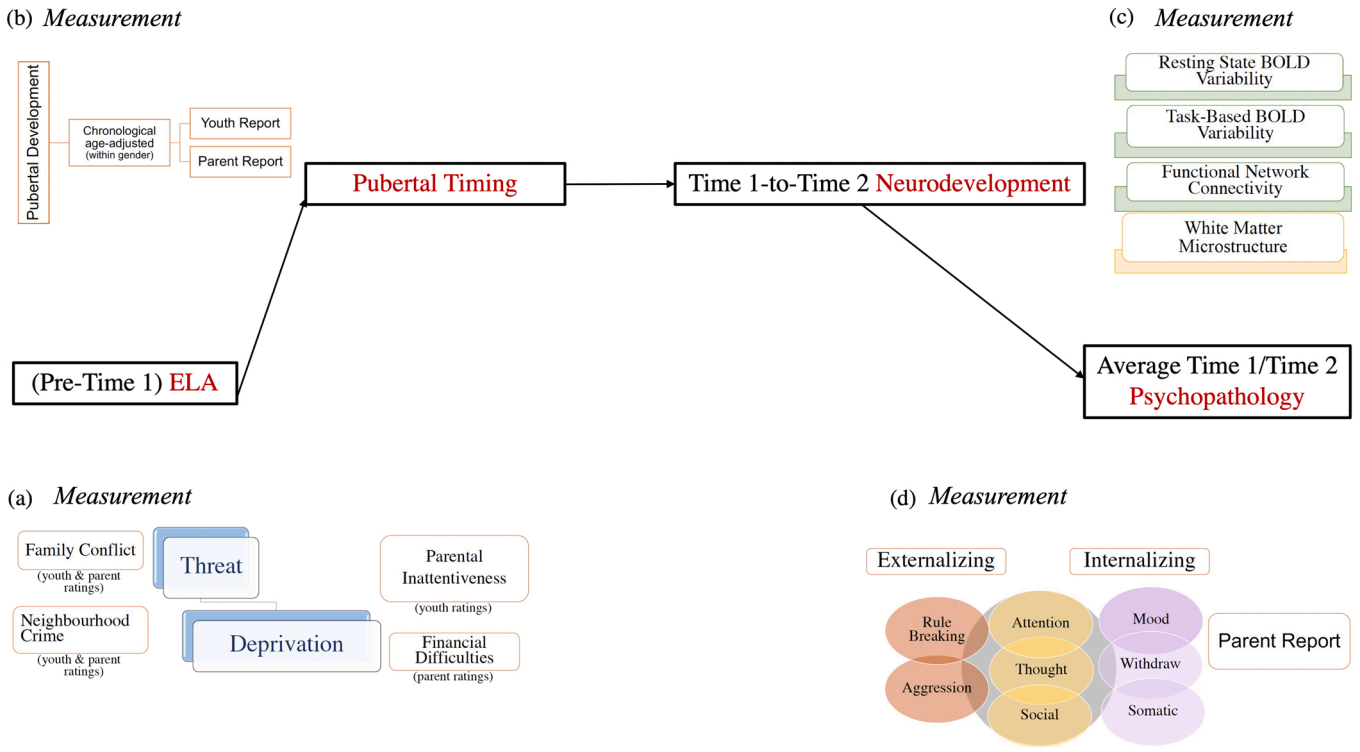

Fig. 1. Outline of the conceptual model with the main measures mapped onto the constructs of interest.

consistent pattern is yet to emerge (Colich et al., 2020a, 2020b). Our main objective was to elucidate whether ELA-linked psychopathology risk stems from yoked alterations in pubertal and structural/functional neurodevelopmental timing (see Fig. 1). A secondary objective was to shed light on the molecular correlates of the ELA-induced neurodevelopmental alterations, thereby identifying potential targets for future pharmacological interventions.

Applying a data-driven multivariate approach to longitudinal Adolescent Brain Cognitive Development (ABCD) data, we estimated the relative contribution of threat- versus deprivation-based ELAs to adolescent psychopathology, defined through eight core syndromes spanning the internalising to externalising spectrum (Funkhouser et al., 2021). Given the impact of family dynamics on child development (Cummings and Miller-Graff, 2015; Harold and Sellers, 2018; Parade et al., 2021) and the increasing motivational salience of the broader social environment from late childhood to adolescence (Crone and Dahl, 2012; Pfeifer and Allen, 2021), we examined whether the degree of sociality would modulate the impact of threat versus deprivation on adolescent psychopathology. We thus sampled ELAs that varied in the extent to which they reflected interpersonal exchanges involving the youth (Zucker et al., 2018 ;Zucker et al., 2018). Perceptions of family conflict and (reverse-coded) parental attentiveness/monitoring captured higher, whereas perceived neighbourhood crime and material hardship reflected lower sociality threat and deprivation, respectively (cf. Zucker et al., 2018; Zucker et al., 2018), *Social Interaction Domain* versus *Proximal [Social] Environment,* Cummings et al., 2014). The ELA profile thus identified was tested for its relevance to earlier pubertal timing (e.g., menarche [girls]), and, indirectly, potentially through the associated hormonal milieu, to earlier-than-expected (based on chronological age) structural and functional neurodevelopment, an effect that was further probed for its psychological domain specificity (i.e., social versus non-social processing, cf. Laube et al., 2020).

Our primary index of whole-brain functional development was BOLD fMRI signal variability [$BOLD_{SV}$] due to its relevance to optimal neural organisation (i.e., network segregation/integration balance) and cognitive-affective functioning, its substantial trait-like variability but also its susceptibility to change across the lifespan (Millar et al., 2020b; Thompson et al., 2021; Waschke et al., 2021). To test our predictions regarding the functional neurodevelopmental impact of ELA, we estimated $BOLD_{SV}$ during wakeful rest and three task contexts varying in sociality and motivational salience (i.e., inhibitory control, monetary reward/punishment, happy/fearful face processing). These tasks tap mental processes with substantial neurobehavioural overlap in adolescence (Crone and Dahl, 2012; Jia et al., 2020), which are also highly susceptible to ELA and predictive of psychopathology risk (Dennison et al., 2016; Grahek et al., 2019; Hanson et al., 2015, 2017; Ironside et al., 2018; Kasparek et al., 2020; McTeague et al., 2017; Tozzi et al., 2020).

Across the lifespan, BOLDsv patterns have been linked to profiles of white matter (WM) microstructure, which, in turn, are vulnerable to ELA, both globally and in a more regionally and ELA type-specific (i.e., threat vs deprivation) manner (Banihashemi et al., 2021; Burzynska et al., 2015; Easson & McIntosh, 2019; Johnson et al., 2021; Wang et al., 2021). Consequently, to estimate correspondence in ELA-linked effects on structural and functional brain maturation, we compared developmental alterations in regionally specific profiles of task-free and/or task-evoked BOLDsv with those observed in the corresponding WM microstructural profiles.

BOLDsv underpins the development and maintenance of functionally segregated brain architecture, a key contributor to optimal cognitive-affective processes, which emerges gradually over the first two decades of life through exposure to task-relevant contexts and tends to decline from late middle-age onwards (Baracchini et al., 2021; Chan et al., 2014; Gabard-Durnam et al., 2016; Geng et al., 2021; Grayson and Fair, 2017; Vakorin et al., 2011; Wig et al., 2011). Income-based ELAs accelerate the emergence of functionally segregated brain networks in adolescence and their decline in late middle age (Chan et al., 2018; Tooley et al., 2020). Consequently, network segregation rate constituted our second index of functional brain maturation, which we investigated for liability to ELA and associations with ELA-linked changes in BOLDsv and WM microstructure profiles. These analyses focused on network-specific indices in order to determine whether ELA would

impact differently the segregation rate of networks varying in their relevance to social information processing.

Finally, to characterise potential molecular-level intervention targets, we estimated the gene expression profiles associated with typical and ELA-induced macroscale neurodevelopmental patterns. To this end, we used the comprehensive transcriptional maps provided by the Allen Institute of Brain Science, an approach successfully adopted by prior adolescent neurodevelopment studies (Ball et al., 2020; Park et al., 2021; Whitaker et al., 2016).

1. Method

1.1. Participants

The sample included participants in the ongoing Adolescent Brain Cognitive Development (ABCD) study which recruited approximately 11,000 youths and their parents/guardians across 21 US data acquisition sites using multi-stage probability sampling (for a detailed sample description, see Garavan et al., 2018). Participants had been selected to capture the variation in age, sex, ethnicity, socioeconomic status (household income), and urbanicity present in the US population.

The present research uses data preprocessed by the ABCD study team and downloaded in December 2020 as part of the ABCD Study Curated Annual Release 3.0 (https://data-archive.nimh.nih.gov/abcd). This release contains longitudinal neuroimaging data from 5685 participants, of whom 4792 are biologically unrelated (i.e., not siblings). Following the recommendations of the ABCD study team (as detailed in the "abcd_imgincl01" file included in the data release), 1514 (747 female) study participants were selected on the basis of being biologically unrelated and having contributed high-quality data on all measures of interest at both baseline (T1) and two-year follow-up (T2). Participants were aged 9–10 years at baseline (M = 120.14 months, SD = 7.38) and 11–12 years at follow-up (M = 144.00 months, SD = 7.62). The majority were predominantly right-handed (N = 1218). Based on parent reports, the racial background of the sample was as follows: White (84.5% [youths] and 82.8% [parents/guardians], respectively), African-American (11.4% [youths] and 8.5% [parents/guardians], respectively) and Other and/or Mixed Race (4% [youths] and 8.7% [parents/guardians], respectively).

1.2. Out-of-scanner measures

All measures described below were completed at both baseline and two-year follow-up (see Fig. 1 for an outline of all measures mapped onto the constructs of interest). Table S1 contains the correlations among all the Time 1 and Time 2 behavioural measures.

1.2.1. ELA

1.2.1.1. Deprivation. Perceived parental inattentiveness. A 5-item Parental Monitoring Scale was completed only by the youth and used as an inverse measure of parental inattentiveness (Chilcoat and Anthony, 1996). This instrument uses a 5-point Likert-type response format, ranging from *1* (*never*) to *5* (*almost always*), in order to assess parents' active efforts to keep track of their children's whereabouts, both at home and outside the home (e.g., "How often do your parents know where you are?"). The five items are assumed to assess distinct aspects of parental monitoring (Zucket et al., 2018), hence a reliability index is not really appropriate for this scale (Clark and Watson, 1995). To facilitate interpretation of results, participants' aggregate scores on this measure were standardised, then multiplied by (−1), so that higher values would indicate greater interpersonal deprivation (i.e., parental inattentiveness).

Material deprivation. Financial deprivation was assessed with a 7-item scale developed by Diemer et al. (2012) to assess unmet material needs in the areas of housing, food and medical care in the 12 months preceding assessment. Each item is scored as *1* or *0* (*yes/no*) with higher scores indicating greater financial hardship (Cronbach's alphas of.73). At the time of writing, only baseline financial deprivation scores were available. Nonetheless, we favoured this measure over income-based indicators of deprivation because we regarded it as being more closely linked to *experiences* of material hardship. As expected, among the 1441 participants with available data on both measures, experienced material deprivation was inversely correlated with the combined household income, Spearman's $rho = -0.42$, $p = 0.0001$.

1.2.1.2. Threat. Both measures of threat-related ELA described below were completed independently by the parent and the youth as part of the wider PhenX Toolkit (Stover et al., 2010). Youth and parent reports were significantly correlated (*r*s from.18 to.30, all *p*s < 0.0001). Thus, in order to minimise individual rater bias, we averaged the child's and parent's ratings in order to create threat indices capturing their shared perception of family conflict and neighbourhood crime, respectively. Nonetheless, in supplemental analyses (see Figs. S2-S5), we verified that all the reported effects are replicated if using the individual youth and parent ratings. We should underscore that the difference between social interaction-varying forms of threat, as operationalised here, is likely to reflect mainly the psychological distance of other social actors who may pose a danger to the self (i.e., proximal, enduring and well-defined [family members] versus distal and "indistinct" [people in one's neighbourhood]) (Bronfenbrenner and Evans, 2000).

Family conflict. The 9-item Family Conflict subscale of the Moos Family Environment Scale (Moos and Moos, 1994) gauged exposure to domestic violence. Each item is scored as *1* or *0* for *true/false*, with reverse coding of items that imply lack of conflict in the home (e.g., "We fight a lot in our family." versus "Family members rarely become openly angry."). Higher scores indicate a more conflictual family environment. One parent/guardian failed to complete the family conflict measure at follow-up, whereas one youth failed to complete it at baseline. In both cases, the missing value was replaced with the rating available at the other time point. Both parent (Cronbach's alphas of.68 and.70) and youth (Cronbach's alphas of.60 and.61) versions demonstrated acceptable reliability.

Perceived neighbourhood crime and safety. The 3-item Neighbourhood Safety/Crime Scale uses a five-point Likert Scale (*5* = *strongly agree* to *1*= *strongly disagree*) to gauge perceptions of threat related to the neighbourhood in which the respondent resides (i.e., areas within a 20-minute walk from the respondent's home, Echeverria et al., 2004). At both time points, the youth completed only a 1-item version of the scale ("My neighbourhood is safe from crime."), whereas the parent filled out the full 3-item version of the scale (Cronbach's alphas of.87 and.86). Higher scores on this scale indicate greater neighbourhood safety. Two youths failed to complete this measure at baseline and one parent/guardian failed to complete it at follow-up. In all cases, the missing value was replaced with the rating available at the other time point. To facilitate interpretation of results, youths' and parents' aggregate scores on this measure were standardised, then multiplied by (−1), so that higher values would indicate greater neighbourhood crime, as perceived by the youths and parents, respectively.

1.2.2. Biological aging

Pubertal development. Pubertal status was assessed with the 5-item Pubertal Development Scale (PDS), which was selected due to its significant correlation with other indices of pubertal development, including physician ratings (Petersen et al., 1988). The questionnaire comprises three gender-general items (i.e., growth spurt, changes in skin, hair growth) and two gender-specific items (e.g., facial hair growth, voice change [boys]; breast development, menarche [girls]). The instrument, which uses a 4-point Likert type response format, ranging from 1 (no development) to 4 (development already completed), was completed separately by the youth and their

guardian/parent. In line with existing practices in the literature (Owens et al., 2021), parent and youth ratings (average r of.68, $p < 0.0001$) were averaged in order to obtain a more robust estimate of pubertal development at baseline and the two-year follow-up, respectively. An index of accelerated pubertal development was computed at each time point by regressing from the aggregate PDS score the youth's biological age, such that a positive residual score indicated accelerated biological aging relative to chronological age (cf. Colich et al., 2020a, 2020b; Sumner et al., 2019). This accelerated pubertal development index was residualised for biological sex (together with other confounding variables detailed in section "Residualization for Confounding Variables" below), thereby controlling for well-documented sex-related differences in pubertal onset (Juraska and Willing, 2017; Marshall and Tanner, 1969, 1970).

1.2.3. Psychopathology symptoms

Child Behavior Checklist (CBCL). The parent-report version of the CBCL was used to index youth psychopathology (Achenbach, 2009). The CBCL consists of 112 items scored on a 3-point Likert scale (0 = Not True, 1 = Somewhat or Sometimes True, 2 = Very True or Often True). Cross-diagnostic symptomatology was quantified via the eight empirically derived problem scales in the CBCL (i.e., anxious/depressed, withdrawn/depressed, somatic complaints, social problems, thought problems, attention problems, rule-breaking, and aggressive behaviour).

1.3. In-scanner tasks

1.3.1. Monetary incentive delay (MID) task

This task gauges anticipatory and consummatory reactions to rewards and losses, as well as motivation to engage in speeded responses for monetary gains or avoidance of losses (Casey et al., 2018), Knuston et al. (2000).

Each trial begins with a monetary incentive cue (duration 2000 ms) of five possible types (Win $.20, Win $5, Lose $.20, Lose $5, $0-no money), followed by a variable (1500–4000 ms) anticipation period. Subsequently, a target appears (150–500 ms) to which the participant responds to win/avoid losing money, followed by feedback on the outcome of the trial (2000 ms – target duration). Each run contains 50 contiguous trials (10 of each type), presented in pseudorandom order, for a total of 40 reward, 40 loss and 20 no-money trials across the two task runs. Task parameters are adjusted for each individual participant in order to maintain an overall accuracy of 60% (Casey et al., 2018).

1.3.2. Emotional N-back (EN-back)

This task is a variant of the n-back task designed to engage both memory and emotion regulation processes (Barch et al., 2013; Schweizer et al., 2019). The task consists of two runs of 8 blocks each. In each run, there were four 2-back blocks, in which participants were asked to respond "Match" if the presented stimulus was the same as the one displayed two trials back, and four 0-back blocks, in which participants were instructed to respond "Match" if the present stimulus was the same as the target stimulus displayed at the beginning of the block. The task commenced with a 2.5 s cue to indicate task type, and, for the 0-back blocks only, an image of the target was also presented. Prior to each block instruction, a 500 ms coloured fixation cross was presented to alert the child to the change of task condition.

Within each run there were 4 fixation blocks (15 s each) and 8 task blocks. Within each task block there were 10 trials (2.5 s each). A trial started with the image of a stimulus displayed for 2 s, immediately followed by a fixation cross (500 ms). Two out of 10 trials in each block were targets, 2–3 were non-target lures and the rest were stimuli only presented once (non-lures). There was a total of 160 trials comprised of 96 unique stimuli of 4 stimulus types: place stimuli drawn from existing studies (Kanwisher, 2001; O'Craven & Kanwisher, 2000; Park and Chun, 2009), and neutral, happy and fearful faces obtained from the NimStim emotional stimulus set (Tottenham et al., 2009) and the racially Diverse Affective Expressions (RADIATE) stimuli set (Conley et al., 2017), accounting for the racial diversity amongst participants. Each of the 4 stimulus types were presented in separate blocks for a total number of 20 trials across the two memory loads.

1.3.3. Stop signal task (SST)

This task measures the ability to inhibit an ongoing speeded motor response to a "Go" signal (Logan, 1994). Although criticisms of this task have surfaced, the key ones have been mostly rectified in the latest data release, which has been used for the present analyses, while the remaining ones pertain primarily to behavioural analyses of the data, which go beyond the scope of the present report (Bissett et al., 2021; Garavan et al., 2021).

The ABCD version of the SST comprises two runs of 180 trials each: 150 "Go" trials, 15 "Stop" trials expected to be unsuccessful and 15 "Stop" trials expected to be successful. To maintain the breakdown of the successful/unsuccessful "Stop" trials, a tracking algorithm was implemented to alter the interval between the presentation of the 'Go stimulus' and the onset of the 'Stop' signal based on the participant's performance. Each run was restricted to begin with a 'Go' trial and stop trials were separated by a minimum of one 'Go' trial.

Each trial lasted 1000 ms and began with the presentation of a black rightward- (50% of the time) or leftward-facing arrow ('Go stimulus') displayed on a mid-grey background. Participants were asked to indicate the arrow direction "as quickly and accurately as possible" using a response panel consisting of two buttons. Participants used their dominant hand to respond to the 'Go' stimuli and this was mapped congruently with handedness. On 'Stop' trials the 'Go' stimulus was unpredictably followed by a 'Stop' signal in the form of an upward facing arrow presented for 300 ms, which indicated to the participants that they should inhibit their response to the previously presented 'Go' signal. The presentation of the "Go" (on the "Go" trials) and "Stop" cue was followed by a fixation cross varying in duration based on participant's reaction time for a total trial duration of 1000 ms.

1.4. fMRI data acquisition

Scanning was performed across 21 US sites, with a protocol harmonised for Siemens Prisma, Philips, and GE 3 T scanners (for details, see (Casey et al., 2018)), Hagler et al. (2019). The analyses reported here are based on the tabulated structural (sMRI), diffusion (dMRI) and functional magnetic resonance imaging (fMRI) data collected on Siemens Prisma and GE 3 T scanners. Scanner type was controlled for in all analyses by using site id as a covariate to account for magnet and sociodemographic differences among sites (Rosenberg et al., 2020). The dMRI data were acquired with a multiband EPI sequence (TR=4100 ms, TE=88[Siemens]/81.9[GE] ms, flip angle=90°, FOV = 240 × 240 mm, 81 slices of 1.7 × 1.7 mm in-plane resolution, 1.7 mm thick, multiband acceleration factor of 3, 96 diffusion directions, seven b = 0 frames and four b-values [(6 directions with b = 500 s/mm^2, 15 directions with b = 1000 s/mm^2, 15 directions with b = 2000 s/mm^2, and 60 directions with b = 3000 s/mm^2)]). T1-weighted were acquired with an MPRAGE-PMC (Prospective Motion Correction) sequence (TR=2500 (Siemens/GE) ms, TE= 2.88 (Siemens)/2 (GE) ms, flip angle= 8°, FOV = 256 × 256 mm, 176 (Siemens)/208 (GE) slices of 1 × 1 mm in-plane resolution, 1 mm thick). The fMRI data were acquired with a multiband EPI sequence (TR=800 ms, TE=30 ms, flip angle=52°, FOV = 216 × 216 mm, 60 slices of 2.4 × 2.4 mm in-plane resolution, 2.4 mm thick, multiband acceleration factor of 6).

Four RS fMRI scans (eyes open with passive crosshair viewing), lasting 20 min in total, were collected in order to ensure at least 8 min of low-motion data. Two runs of each task were also acquired for a total duration of 10:44 (MID), 9:40 (EN-back) and 11:40 (SST) minutes, respectively (Hagler Jr. et al., 2019).

1.5. fMRI data preprocessing

Our analyses used tabulated dMRI and fMRI data available as part of the ABCD Study Curated Annual Release 3.0. Variables derived from the sMRI data were only used as controls. The main processing steps applied to these data by the ABCD study team are outlined below (for further details, see Hagler Jr. et al., 2019).

1.5.1. dMRI

Eddy current distortion correction was applied along the phase-encode direction using nonlinear distortion estimation based on diffusion gradient orientations and amplitudes. Robust diffusion tensor estimation was used to identify and replace (through interpolation) dark slices caused by abrupt head motion (Chang et al., 2005). To correct for head motion, each frame was rigid-body registered to the corresponding volume obtained from the post-eddy current corrected censored tensor fit (Hagler et al., 2009). Further processing steps included: adjustment of the diffusion gradient matrix for head rotation (Hagler, et al., 2009; Leemans and Jones, 2009); correction of spatial distortions using the reversing gradient method (Andersson et al., 2003; Smith et al., 2004), as well as adjustment of gradient non-linearity distortions for each frame (Jovicich et al., 2006). The T_2-weighted b= 0 images were registered to the T_1-weighted structural images using mutual information (Wells et al., 1996), after which dMRI images were resampled into a standard space with 1.7 mm isotropic resolution.

WM microstructural properties were quantified using conventional diffusion tensor imaging (DTI) methods, specifically, standard linear estimation methods with log-transformed diffusion-weighted signals (Basser, et al., 1994; Pierpaoli, et al., 1996). Our analyses featured the output of the DTI full shell model, specifically, average estimates of fractional anisotropy (FA), as well as radial (RD) and longitudinal (LD) diffusivity associated with the white matter adjacent to the cortical ROIs from the Destrieux anatomical atlas (Destrieux et al., 2010).

1.5.2. fMRI

Preprocessing of all functional images involved correction for head motion (Cox, 1996), spatial and gradient distortions (Andersson et al., 2003; Jovicich et al., 2006), bias field removal, elimination of initial volumes (8 volumes [Siemens], 5 volumes [GE DV25], 16 volumes [GE DV26]) to allow the MR signal to reach steady state equilibrium, normalisation of the voxel time series and co-registration of the functional images to the participant's T_1 _ weighted structural image. Linear regression was subsequently used to remove from each voxel's time course quadratic trends, as well as the six motion parameters, their first derivatives, and squares (24 motion terms in total; Power et al., 2015; Satterthwaite et al., 2013). Estimated motion time courses were filtered to attenuate signals related to respiration (Fair et al., 2020).

1.5.2.1. Resting-state (RS). The following preprocessing steps were specific to the RS data (1) regression of the mean time courses of cerebral WM, ventricles, whole brain, and their first derivatives, (2) bandpass filtering of the residual time series between.009–0.08 Hz; exclusion of (3) time points with framewise displacement (FD) greater than 0.20 mm, (4) those that were outliers in standard deviation (SD) across ROIs (i.e., SD > three times the median absolute deviation below or above the median SD for a given participant), and of (5) time periods with fewer than 5 contiguous volumes with FD smaller than 0.20 mm.

Temporal variance. Based on the preprocessed data, averaged time courses were computed for cortical ROIs from an anatomically defined parcellation (Destrieux et al., 2010; Fischl et al., 2002), as well as for cortical ROIs from a widely used functionally defined parcellation based on resting state connectivity patterns (Gordon et al., 2016). Temporal variance was estimated for each ROI as an amplitude index of low frequency fluctuations, which is assumed to reflect spontaneous neural activity and is predictive of task-related responsiveness (Fox et al., 2007; Mennes et al., 2011; Zou et al., 2013).

Functional network segregation. Pairwise Pearson's correlations between all the ROIs in the Gordon atlas were computed and expressed as Fisher's z-transformed scores. Our analyses included only the ROIs that were affiliated with a specific functional network in Gordon et al. (2016), such as auditory (AUD), cingulo-opercular (CON), cingulo-parietal (CP), default mode (DMN), dorsal attention (DAN), frontoparietal (FPC), retrosplenial (RSP), sensorimotor-hand (SM-hand), sensorimotor-mouth (SM-mouth), salience (SAL), ventral attention (VAN) and visual (VIS). Based on the functional network labels provided by these authors, summary measures of within-network (e.g., the average correlation among all the DMN ROIs) and between-network (e.g., the average correlation of all the DMN ROIs with the ROIs from all remaining networks) connectivity were created by averaging all relevant ROI-to-ROI correlation indices. To compare developmental changes in within- versus between-network connectivity, we used the same segregation index as Chan et al. (2014, 2018):

System segregation = Z_{w}- $Z_b/Z_{w,}$

where Z_w is the average connection strength among all the nodes within a network to which a constant ("1") has been added to render it positive and Z_b is the average connection strength between nodes in one network and nodes in all the remaining networks to which the same.

constant ("1") has been added to render it positive.

1.5.2.2. Task. The following preprocessing steps were specific to the task data: (1) regression of the baseline, and (2) removal of time points with FD > 0.90 mm. Task-specific activation strength was estimated for each individual participant using a general linear model in AFNI's 3dDeconvolve (Cox, 1996). The baseline model ("null model") included regressors for average signal, quadratic trend and motion (i.e., 24 motion regressors in total, specifically, the linear and quadratic motion parameters and their derivatives). The GLM for each task included the stimulus time series convolved with the hemodynamic response function (HRF). The latter was modelled with a gamma variate function and its temporal derivative in AFNI's SPMG option within 3dDeconvolve. Events were modelled as instantaneous for the SST and MID analyses. In the EN-back, the cue trials (~3 s) and task blocks (~24 s) were modelled as square waves convolved with the two-parameter HRF (Hagler Jr. et al., 2019).

Task-related variability. Our analyses of task-related variability focused on the average standard error (SEM) of the GLM beta coefficients estimated across the two runs of each task for each of the ROIs in the Destrieux anatomical atlas, with lower SEM values indicating a more consistent response to the task-relevant information. The SEMs of interest involved the following linear contrasts: 'social reward' (happy faces > neutral faces [baseline]) and 'threat' (fearful faces > neutral faces [baseline]) in the EN-back task, anticipation of non-social reward (> neutral anticipation [baseline]) and loss (> neutral anticipation [baseline]) in the MID task, as well as successful inhibition (correct Stop > correct Go [baseline]) in the SST task.

1.5.3. sMRI

The sMRI preprocessing pipepline included removal of non-brain tissue, corrections for gradient non-linearity distortions and intensity inhomogeneity, intensity normalisation, as well as rigid resampling and alignment to an averaged brain image in standard space. Cortical reconstruction and subcortical segmentation were performed using FreeSurfer version 5.3, where estimates of cortical thickness and volume were computed for each of the 148 ROIs from the Destrieux atlas.

1.6. Gene expression data processing

1.6.1. Microarray gene expression

Micro-array gene expression data were obtained from six postmortem brains (1 female, ages 24.0–57.0, 42.50+/- 13.38 years) provided

by the Allen Institute for Brain Science (https://www.brain-map.org/). Because only two of the six brains contained data from the right hemisphere and the nature of our brain-expression analyses rendered problematic averaging across the two hemispheres, our gene expression analyses were conducted only on the left hemisphere ROIs (cf. Ball et al., 2020; Hansen et al., 2021). The gene expression data was processed with abagen (https://github.com/netneurolab/abagen). Microarray probes were reannotated based on Arnatkevičiūtė et al. (2019) and filtered based on their expression intensity relative to background noise (Quackenbush, 2002), such that probes with intensity less than the background in > =50% of samples across donors were discarded. When multiple probes indexed the expression of the same gene, we selected and used the probe with the most consistent pattern of regional variation across donors (i.e., differential stability; Hawrylycz et al., 2015), calculated with:

$$\Delta_s(p) = \frac{1}{\binom{N}{2}} \sum_{i=1}^{N-1} \sum_{j=\, i+1}^{N} \rho\left[B_i(p), B_j(p)\right]$$

where *p* is Spearman's rank correlation of the expression of a single probe, p, across regions in two donor brains *Bi* and *Bj*, and N is the total number of donors. Here, regions correspond to the structural designations provided in the ontology from the AHBA.

The MNI coordinates of tissue samples were updated to those generated via non-linear registration using the Advanced Normalization Tools (ANTs; https://github.com/chrisfilo/alleninf). Samples were assigned to brain regions in the Destrieux atlas if their MNI coordinates were within 2 mm of a given parcel. All tissue samples not assigned to a brain region in the provided atlas were discarded.

Inter-subject variation was addressed by normalising tissue sample expression values across genes using a robust sigmoid function (Fulcher et al., 2013):

$$X_{\text{norm}} = 1/(1+\exp(-(x-\langle x\rangle)/\text{IQR}_x))$$

where $\langle x\rangle$ is the median and IQR*x* is the normalised interquartile range of the expression of a single tissue sample across genes. Normalised expression values were then rescaled to the unit interval:

$$x_{scaled} = (x_{norm} - \min(x_{norm}))/(\max(x_{norm}) - \min(x_{norm}))$$

Gene expression values were then normalised across tissue samples using an identical procedure. Samples assigned to the same brain region were averaged separately for each donor and then across donors. This analysis yielded a 74 (ROIs) x 15,633 (genes) regional expression matrix, which was used in all the gene-neurodevelopment PLS analyses described below. Two ROIs were eliminated because they did not have any gene expression data, leaving 72 ROIs in the analyses reported below.

1.6.2. Gene ontology (GO) enrichment analysis

To link gene expression profiles to relevant biological processes, we used the online tool GOrilla (http://cbl-gorilla.cs.technion.ac.il, version 6 March 2021; single ranked list of genes, Eden et al., 2007, 2009) to search for enriched GO terms linked to the genes with the highest loading on our partial least squares (PLS) LVs (see behavioural PLS on gene expression-neurodevelopment described below). For these analyses, we unchecked the "Run GOrilla in fast mode" option and used the "P-value threshold 10^{-5}" in the advanced parameter settings. FDR values are provided for each GO term in the Supplemental Materials. For each PLS LV (typical vs. ELA-linked neurodevelopment), separate analyses were run for ranked lists featuring genes with reliable positive vs negative loadings. Subsequently, we used REViGO (http://revigo.irb.hr, Supek et al., 2011) to eliminate redundant GO terms and keep only those with medium semantic similarity. The remaining lists of GO terms corresponding to each relevant PLS LV are represented as word clouds (based on the frequency of the GO terms) in Figs. 2 and 5.

1.7. fMRI and gene expression data analysis

1.7.1. Partial least squares analysis (PLS)

To provide a comprehensive description of developmental changes in BOLD_{sv} and WM microstructural properties, as well as characterise the relationship between brain maturation and gene expression profiles, we used partial least squares correlation often referred to as *PLS* (Krishnan et al., 2011), a multivariate technique that can identify in an unconstrained, data-driven manner, neural patterns (i.e., latent variables or LVs) related to different conditions (i.e., task PLS) and/or individual differences variables (behavioural PLS). PLS was selected to characterise typical and ELA-linked neurodevelopmental changes because, unlike other multivariate data reduction techniques (e.g., canonical correlation analysis), it performs well with datasets containing highly correlated variables and in which the number of variables exceeds the number of cases McIntosh & Mišić (2013). PLS was implemented using a series of Matlab scripts, which are available for download at https://www.rotman-baycrest.on.ca/index.php?section = 345.

1.7.1.1. Neurodevelopment: Task PLS. We conducted a sole task PLS analysis in order to identify yoked developmental changes in profiles of WM microstructural properties, as well as RS and task-evoked BOLD brain signal variability as observed in the Destrieux anatomical ROIs. Because the various data types (FA, LD, RD, RS, n-back-fearful faces, n-back-happy faces, MID-loss, MID-win, SST-Stop) had different ranges and that would have biased the PLS results, we normalised each ROI's scores within each data type by computing the corresponding normalised Euclidean distance and adding the same constant to all the ROI scores across all conditions in order to render them positive. In this PLS analysis, each type of data (as listed above) was modelled as a separate group and each time point as a separate condition within each group. Within each "group", the brain matrix contained the participants' concatenated scores for the respective data type across the 148 Destrieux ROIs at baseline and two-year follow-up, respectively. The design matrix contained a number of dummy coded variables corresponding to each condition/time point within each group/type of data (e.g. baseline FA scores). By entering both time points and all nine data "groups" within the same PLS analyses we were able to identify synchronous developmental changes in function and structure. We verified that the within-data group standardisation of each ROI's scores did not bias the results by running task-PLS analyses on raw data, separately for each data type (i.e., dMRI, task fMRI, resting state fMRI), and confirming that the obtained results were consistent with those resulting from the combined analyses herein reported.

1.7.1.2. ELA-related neurodevelopmental changes: Behavioural PLS. To identify yoked developmental changes in profiles of BOLDsv and WM microstructural properties, which are linked to ELA and risk for psychopathology, we conducted a behavioural PLS analysis. The brain matrix was identical to the one entered in the task PLS analysis described above. The baseline ELA (entered at both time points) and the corresponding psychopathology profiles at baseline and follow-up, as estimated with canonical correlation analyses (CCAs, see below), were entered as the behavioural variables.

1.7.1.3. Gene expression-typical/ELA-linked neurodevelopment associations: Behavioural PLS. To probe the link between gene expression profiles and patterns of typical versus ELA-related neurodevelopment, we conducted two behavioural PLS analyses. In the first analysis, the "behavioural" variables were the two pattern scores of typical structural and functional neurodevelopment, as characterised in the task-PLS. In the second analysis, the "behavioural" variable was the pattern score of ELA-linked structural and functional neurodevelopment, which was estimated in the behavioural PLS analysis described above.

1.7.1.4. Significance and reliability testing. In all the reported PLS analyses, the significance of each LV was determined using a permutation test (5000 permutations for the brain-[behaviour] analyses and 100,000 permutations for all the analyses involving gene expression data). In the permutation test, the rows of the ROI temporal variance/WM properties or of the gene expression data are randomly reordered (Krishnan et al., 2011). In the case of our present analyses, PLS assigned to each ROI a weight, which reflected the contribution of the respective ROI to a specific LV. The reliability of each ROI's or gene's contribution to a particular LV was tested by submitting all weights to a bootstrap estimation (1000 bootstraps for the brain-[behaviour] analyses and 100,000 bootstraps for all the analyses involving gene expression data) of the standard errors (SEs, Efron, 1981) (the bootstrap samples were obtained by sampling with replacement from the participants, Krishnan et al., 2011). In order to increase the stability of the reported results, we used a number of permutations/bootstraps several orders greater than the standard ones (i.e., 500 permutations/100 bootstrap samples), as recommended by McIntosh and Lobaugh (2004) for use in PLS analyses of neuroimaging data. The higher number of permutations/bootstraps used for the gene expression data was determined by the relatively lower result stability compared to the brain-(behaviour) only analyses. A bootstrap ratio (BSR) (weight/SE) of at least 4 in absolute value (approximate associated p-value <0.0001) was used as a threshold for identifying those ROIs or connections that made a significant contribution to the identified LVs. The BSR is analogous to a z-score, so an absolute value greater than 2 is thought to make a reliable contribution to the LV (Krishnan et al., 2011), although for neuroimaging data BSR absolute values greater than 3 are recommended for use (McIntosh & Lobaugh, 2004). The unthresholded BSR values reflecting the contribution of each gene to the identified gene expression LV were used to create the ranked (positive versus negative) list for Gorilla.

1.8. Brain-behaviour analyses

1.8.1. Canonical correlation analysis (CCA)

To identify ELA and brain profiles predictive of psychopathology, we conducted a series of canonical correlation analyses (CCAs, Hotelling, 1936) with cross-validation procedures (cf. Hair et al., 1998). CCA is a multivariate technique, which seeks maximal correlations between two sets of variables by creating linear combinations (i.e., canonical variates) from the variables within each set. Recently, CCA has been successfully used to investigate brain-behaviour relationships in large datasets (see Modabbernia et al., 2021; Smith et al., 2015; Tsvetanov et al., 2016; Wang et al. 2020).

CCA was implemented in Matlab using the canoncorr module. In order to obtain reliable estimates of correlations between the brain or behavioural variables and their corresponding variates, it is generally recommended that CCA be performed on a sample size at least ten times the number of variables in the analysis Hair et al. (1998), a criterion which was exceeded in all analyses reported below.

The performance of our CCA models was tested by using a 10-fold cross validation procedure (as is generally recommended, Hair et al., 1998). For all sets of CCAs, discovery analyses were conducted on nine folds of data and the resulting CCA weights were employed to derive predicted values of the brain and behavioural variate in the left-out ("test") fold. This procedure was repeated until each of the ten folds served as "test" data once. The correlation between the predicted brain and behavioural variates across all testing folds was evaluated using a permutation test with 100,000 samples (cf. Smith et al., 2015). To describe the relationship between the behavioural or brain variables and their corresponding variates across all the testing folds, we include correlations between the observed value of a brain or behavioural variable and the predicted value of its corresponding variate, as well as standardised coefficients, analogous to multiple regression coefficients, which indicate the unique association between the observed value of a behavioural or brain variable and the predicted value of its corresponding variate. The correlation and standardised regression-like coefficients described above are analogous to canonical loadings and canonical weights, respectively (see also Tsvetanov et al., 2016; Vatansever et al., 2017), with the only difference being that they are computed in the test, rather than the discovery, folds and, thus, reflect more conservative effect estimates. Because the brain profiles targeted synchronised developmental changes across multiple levels/modalities, standardised regression-like coefficients are not included for the brain variables. Both discovery and test CCAs were conducted on standardised variables.

1.8.2. Mediation analyses

To test whether pubertal timing and neurodevelopmental changes mediate the effect of ELA on psychopathology, we used Hayes' PROCESS 3.5 macro for SPSS (Hayes, 2018). PROCESS is an ordinary least squares (OLS) and logistic regression path analysis modelling tool, based on observable variables. Mediation models were tested employing 95% CI with 50,000 bootstrapping samples. In line with extant guidelines on balancing Type I and Type II errors in mediation analyses (Hayes and Scharkow, 2013; Tofighi and Kelley, 2020), the CIs for indirect effects was estimated using percentile bootstrap, which is the default option in PROCESS 3.5. As recommended by Hayes and Cai (2007), a heteroscedasticity consistent standard error and covariance matrix estimator was used. Bootstrapping-based 95% CIs for the indirect effects and for the difference between them (cf. Miočević et al., 2018; Walters, 2018), as outputted by PROCESS, were used as effect size estimates.

1.9. Residualization for confounding variables

In line with existing practices (Modabbernia et al., 2021), the following were regressed out from each imaging (ROI-based/functional network-based) and non-imaging variable prior to analyses: (1) sex (coded as "1" for females, "0" for males); (2) race (coded as "0" for White [> 80% of the present sample] and "1" for Non-White); (3) handedness (coded as "0" for right-handedness [> 80% of the present sample] and "1" for non-right-handedness); (4) serious medical problems, which was based on the ABCD (Longitudinal) Parent Medical History Questionnaire and computed as an average of unplanned hospital visits (in the prior year for Time 1, cumulatively across all available time points Time 2) for chronic health conditions, head trauma, loss of consciousness and/or convulsions/trauma; (5) scanner site (20 dummy variables to account for scanner-related differences, as well as broad differences in family education and socio-economic status across sites, cf. Rosenberg et al., 2020). In addition, the following were regressed out only from the dMRI and fMRI data: (1) average modality-specific (dMRI/fMRI) motion per participant (Power et al., 2015); (2) regionally specific (for the ROI data) or participant-specific (for the functional network segregation indices) cortical thickness and volume (see Millar et al., 2020a; Pur et al., 2019, for evidence of cortical thickness/volume effects on BOLDsv). We did not deem it necessary to control for behavioural performance on the in-scanner tasks as we only included well-performing participants (accuracy > 60%) and, on the SST, we only analysed correct trials.

1.10. Supplementary analyses

As an acknowledgement of the fact that some of the variables regressed out as "nuisance" from our core predictors or outcomes could be of interest to other researchers, we report supplemental analyses related to (1) developmental changes in CT and GMV; (2) independent broad replication of the effects reported below within each sex and using separate indices of parental versus youth perceptions of family conflict and neighbourhood crime, respectively (see Figs. S1-S5).

2. Results

2.1. Typical neurodevelopment

2.1.1. BOLDsv and WM microstructure

The task PLS analysis revealed three significant LVs (all *ps* = 0.0002), which explained 72%, 20% and 6.53% of the variance in the data. Below we only discuss the first two extracted LVs, since the third one only identified age-related changes in WM microstructure (i.e., LD/RD), but not BOLDsv.

2.1.1.1. Developmental LV 1. This profile reflected age-related decrements in RD, accompanied by age-related increments in FA, LD, and BOLDsv across both task and rest (see Fig. 2-a). Although reliably observed in 145 of the 148 Destrieux ROIs, this pattern was most strongly expressed in occipital, temporal and parietal areas (see Fig. 2-b).

2.1.1.2. Developmental LV 2. The second LV identified two groups of ROIs showing opposing patterns of increments/decrements in task-related BOLDsv and WM microstructural properties (i.e., FA, LD) (see Fig. 2-c). Thus, after accounting for the brain-wide increase in FA/LD and BOLDsv, as indicated by LV1, there was evidence that frontal and parietal regions demonstrate age-related BOLD signal stabilisation during task performance, which is accompanied by increasing FA and LD, but declining RD (see Fig. 2-d). Complementarily, areas in the cingulate, medial orbital, temporal, including the parahippocampal gyri, as well as the occipito-temporal cortex evidenced age-related increases in BOLDsv and RD together with declines in FA and LD (see Fig. 2-d).

2.1.2. Transcriptional profiles associated with the two BOLDsv/WM microstructure developmental LVs. One behavioural PLS analysis probed the link between expression of the two task-PLS brain LVs (i.e., ROI-specific weights) described above and gene expression in each of the 72 left hemisphere ROIs from the Destrieux ROIs. The analysis identified a single gene LV ($p = 0.0002$, 75% explained covariance) which showed opposing relationships with the two developmental brain LVs, as detailed below.

2.1.2.1. Gene expression signature of the developmental LV1. The developmental brain LV 1 showed a significant positive association with the identified gene LV ($r = 0.55$, 95% CI = [0.40;0.71]). This transcriptional profile was most enriched in genes regulating inorganic cation transmembrane transport ($p = 2 \times 10^{-10}$) and, more broadly, ion transmembrane transport ($p = 4 \times 10^{-8}$), cellular biosynthethic processes ($p = 3 \times 10^{-7}$) and nucleic acid metabolic processes ($p = 3 \times 10^{-7}$). A selection of GO terms most relevant to brain structure/function is represented as a word cloud based on Revigo-estimated frequency in Fig. 2-e. A complete table of the GO terms that passed our significance threshold in Gorilla is part of the Supplemental Materials.

2.1.2.2. Gene expression signature of the developmental LV2. The developmental brain LV 2 showed a significant negative association with the identified gene LV ($r = -0.41$, 95% CI = [−0.22;0.57]). This transcriptional profile was most enriched in genes regulating immune system processes ($p = 10^{-12}$), signal transduction ($p = 10^{-10}$), cell surface receptor signalling pathway ($p = 4 \times 10^{-10}$), localisation ($p = 4 \times 10^{-10}$), exocytosis ($p = 10^{-9}$), response to external stimuli ($p = 8 \times 10^{-9}$), and cell proliferation ($p = 6 \times 10^{-8}$). A selection of GO terms most relevant to brain structure/function is represented as a word cloud based on Revigo-estimated frequency in Fig. 2-f. A complete table of the GO terms that passed our significance threshold in Gorilla is part

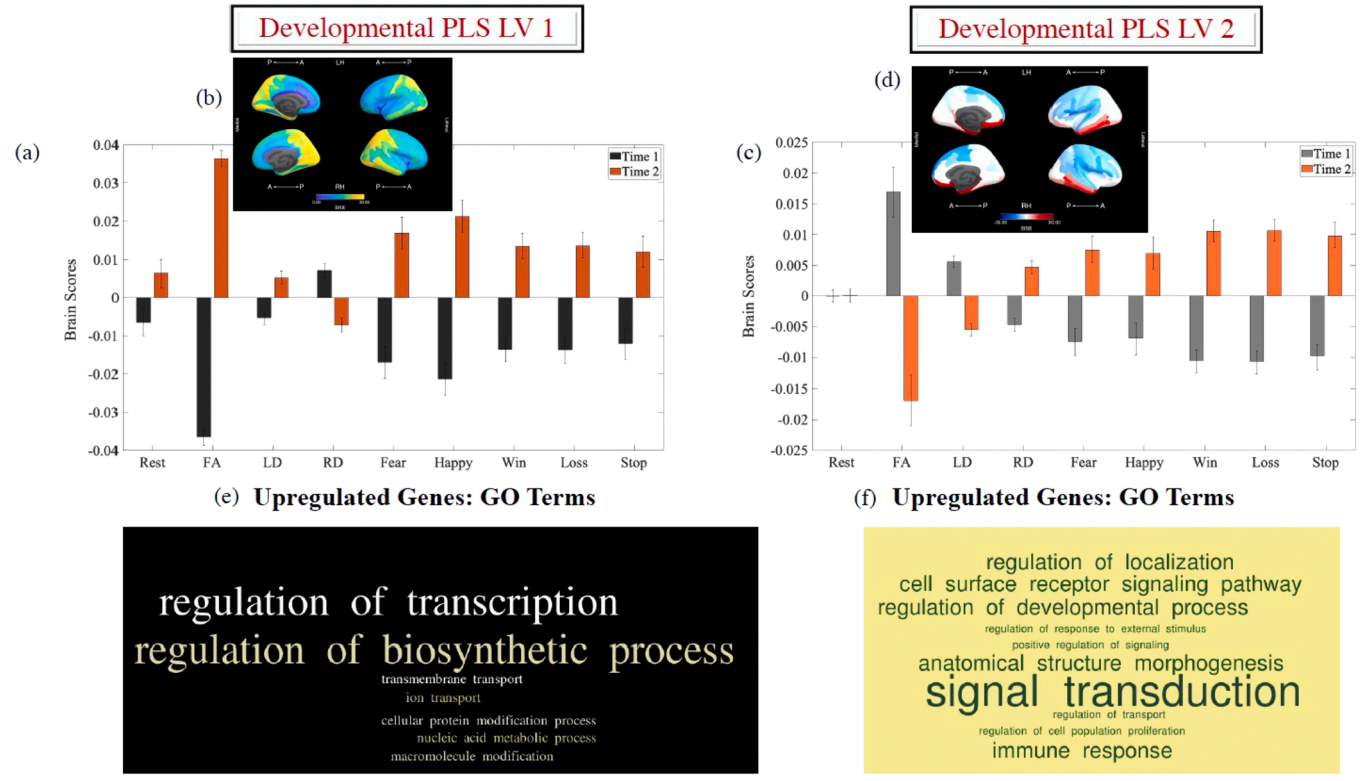

Fig. 2. Results of the task-PLS analysis. The graphs in panels (a) and (c) show the average of the mean-centred LV1 and LV2 brain scores at each time point within each data group (error bars are the 95% confidence intervals [CI] from the bootstrap procedure). Non-overlapping CIs indicate differences between conditions. Panels (b) and (d) depict the Destrieux ROIs with positive loadings and negative loadings on the LVs graphed in panels (a) and (c), respectively, and visualised with the Freesurfer Surface (https://chrisadamsonmcri.github.io/freesurfer_statsurf_display). In the brain figures in panels (b) and (d), absolute BSR values lower than 4 have been set to zero. BSR = bootstrap ratio. LV = latent variable. Panels (e) and (f) depict the GO enrichment terms, which are most relevant to brain function and associated with each of the two developmental LVs.

of the Supplemental Materials.

2.1.3. Age-related changes in WM microstructural properties and patterns of BOLDsv across task and rest predict emergence of canonical functional brain networks. Next, we tested whether expression of the two brain PLS LVs described above predicts segregation rate for the 12 canonical functional brain networks from the Gordon atlas. To this end, we created a difference brain LV score (Time 2 – Time 1) for each of the nine data types entered in the task PLS analysis described above for a total of 17 LV scores across the two LVs (the LV2 difference score for RS was not included because the RS condition did not load robustly on LV2, see Fig. 2-c). To facilitate interpretation and preserve the format of the LVs (Fig. 2-a, c), the LV1 difference score for RD and the LV2 difference scores for FA and LD were multiplied by (−1). Subsequently, we created a difference score reflecting the baseline to follow-up increase in segregation (i.e., within- relative to between-network connectivity) for each of the 12 networks in the Gordon atlas. Ten discovery CCAs were subsequently conducted to probe the link between age-related increases in functional network segregation and age-related increases in the expression of the two developmental brain PLS LVs. Of the extracted CCA modes, only one was validated across all the test folds ($r_{discovery}$ from.30 to.33, all $ps = 10^{-5}$, r_{test} =0.21, $p = 10^{-5}$, see Fig. 3-b). Broadly, this mode linked normative increases in functional brain segregation to developmental changes in brain-wide BOLDsv (i.e., increases during rest, but decreases during task [particularly, reward/loss processing, inhibitory control]) and regionally-specific WM microstructure (i.e., FA/LD decreases in frontal/parietal, but increases in anterior cingulate, medial orbital, temporal and occipital areas) (see Fig. 3-a). The effect of changes in BOLDsv/WM microstructural properties on functional segregation was strongest for networks relevant to environmental vigilance (CON), internally guided cognition (DMN), external attention (DAN, VAN), episodic memory (RSP), auditory processing and top-down cognitive control (FPC) (see Fig. 3-c).

2.2. The impact of ELA on psychopathology risk

2.2.1. Greater baseline family conflict predicts higher psychopathology risk, both concurrently and prospectively; material deprivation exerts an independent, albeit weaker, effect on psychopathology risk. Ten discovery CCAs were conducted to probe the relationship between ELA and psychopathology at baseline. Of the two significant modes thus identified, we describe here only the one that was subsequently found to have a significant link to neurodevelopment. This was the strongest mode emerging from the discovery CCAs and validated across all test folds ($r_{discovery}$ from.33 to.36, all $ps = 10^{-5}$, r_{test} =0.31, $p = 10^{-5}$, see Fig. 4-e). It indicated that, of all the scrutinised ELAs, family conflict has the strongest positive association with psychopathology, specifically, attentional difficulties, aggression, rule breaking, withdrawal and somatic complaints (see Fig. 4-b, d). Importantly, there was evidence that material deprivation exerted an independent, yet weaker, additive effect on psychopathology risk (see Fig. 4-b).

To probe the temporally distal effects of the identified ELA profile, we applied the weights from the baseline discovery CCAs to the two-year follow-up data and computed the respective psychopathology variate scores. Subsequent permutation-based correlational analyses confirmed that expression of the baseline ELA profile predicts maintenance of its associated psychopathology profile at the two-year follow-up (r_{test} =0.26, $p = 2 \times 10^{-5}$, see Fig. 4-f), an effect that was in line with the strong positive correlation between the Time 1 and Time 2 psychopathology profiles (r of.66, $p = 10^{-5}$).

2.2.2. Neural and gene transcription profiles mediating the impact of ELA on psychopathology

2.2.2.1. Alterations in threat processing, together with delayed perceptual, but accelerated attentional/control network segregation predict persistent psychopathology risk associated with ELA exposure. ***BOLDsv/WM microstructural characteristics.*** A behavioural PLS analysis using the baseline ELA, as well as the baseline and follow-up psychopathology profiles characterised above as the behavioural variables identified two LVs, accounting for 50% and 10% of the covariance in the data, respectively. Below, we only discuss the first extracted LV, since the second LV linked both ELA and psychopathology (at either time) only to the WM microstructural variables (LD/FA).

The first extracted brain LV ($p = 0.0002$, see Fig. 5-a) was robustly expressed in 66 of the Destrieux ROIs, but particularly strongly in the insula, as well as occipital, temporal, parietal and inferior frontal areas (see Fig. 5-b). The results indicated that, at Time 1, both psychopathology and ELA exposure correlated with greater brain-wide BOLDsv in response to threat (i.e., fearful faces). Complementarily, at Time 2, concurrent psychopathology and earlier (i.e., [pre]-Time 1) ELA exposure were associated with reduced RS BOLDsv. Of note, although ELA exposure predicted departure from typical WM microstructural development (LD/RD) at both time points, this was not associated with psychopathology (see Fig. 5-a). This is why LD and RD LV scores were not entered in the CCA and mediational analyses probing the role of neurodevelopment in accounting for ELA-associated psychopathology.

ELA-linked effects on gene transcription profiles. A behavioural PLS analysis tested the relationship between expression of the ELA/

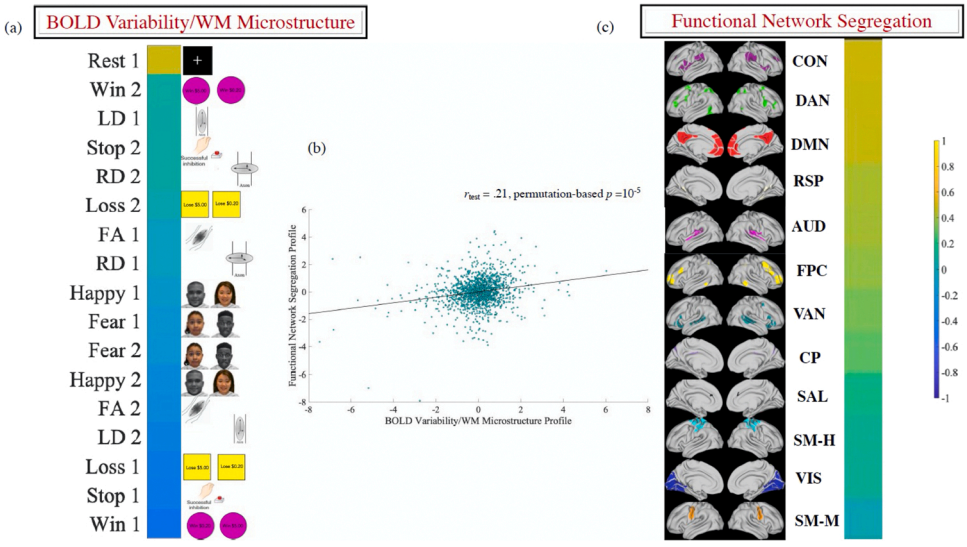

Fig. 3. Results of the CCA linking the neurodevelopmental profiles (i.e., brain LVs) previously identified with task-PLS (panel a) to longitudinal increases in functional network segregation (panel c). The scatter plot in panel (b) describes the linear relationship between the predicted values of the two variates across all test CCAs and is based on standardised variables. The networks in panel (c) have been visualised with the Conncetome Workbench (https://www.humanconnectome.org/software/connectome-workbench). AUD = auditory; CON = cingulo-opercular; CP = cingulo-parietal; DMN = default mode; DAN = dorsal attention; FPC = frontoparietal; RSP = retrosplenial/temporal; SM-H = somatomotor-hand; SM-mouth = somatomotor mouth; SAL = salience; VAN = ventral attention; VIS = visual. LV = latent variable. WM = white matter.

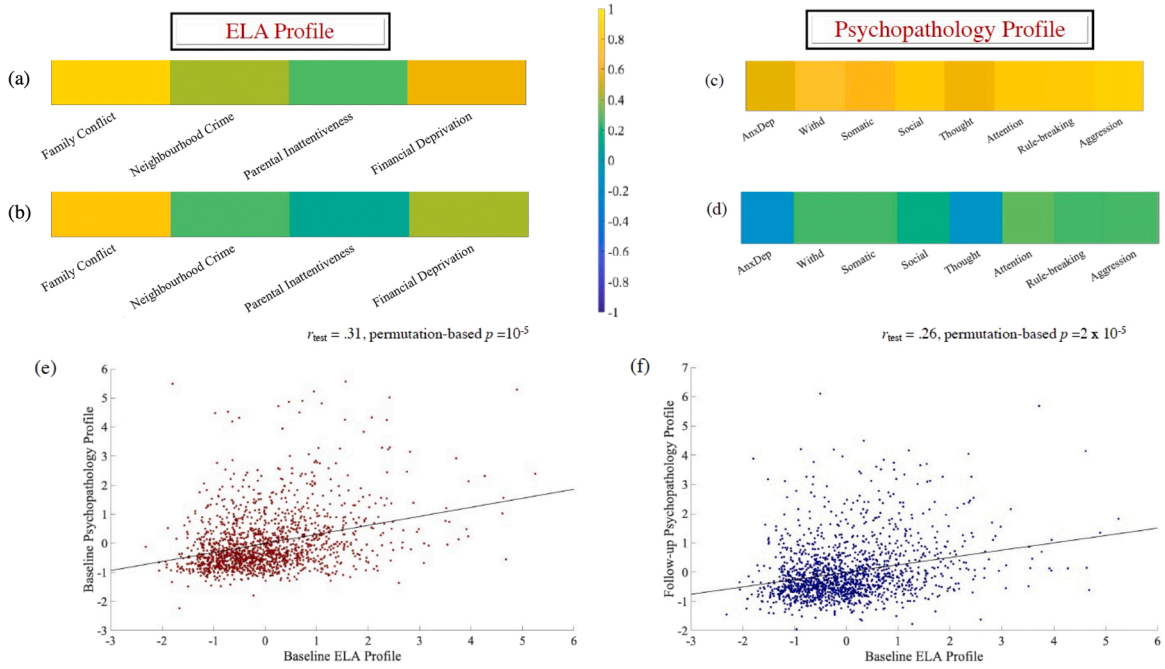

Fig. 4. The relationship of Time 1 ELA with Time 1 and Time 2 psychopathology. Correlation [panels a, c] and standardised coefficients [panels b, d] describing the relationship between the observed variables and the predicted value of their corresponding canonical variate ("profile") across all test CCAs. The scatter plots in panel (e) and (f) describe the linear relationship between the predicted values of the two variates ("profiles") across all test CCAs and are based on standardised variables. ELA = early life adversity. AnxDep = Anxiety/Depression. Withd = Social Withdrawal. Somatic = Somatic Complaints.

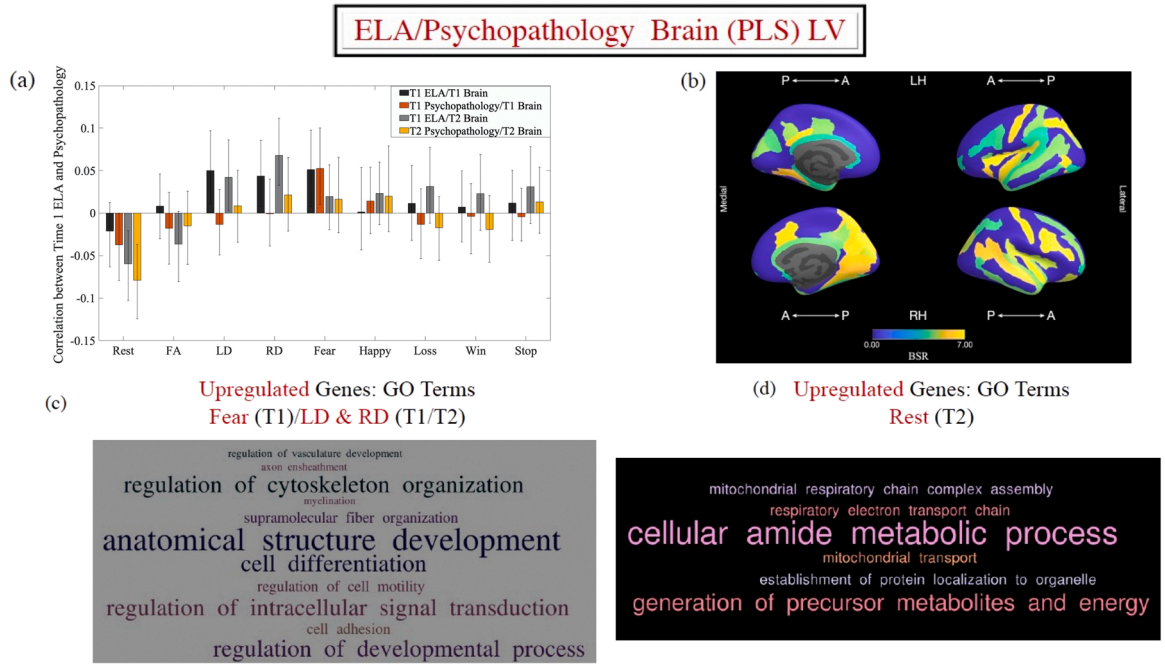

Fig. 5. Results of the behavioural-PLS analysis linking baseline ELA/concurrent psychopathology to the $BOLD_{SV}$/WM microstructure variables (panel a). Panel (a) shows the correlations between the LV brain scores and the ELA-Psychopathology variate scores (previously estimated with CCA, as described in the main text). Error bars are the 95% CIs from the bootstrap procedure. CIs that do not include zero reflect robust correlations between the respective behavioural variable and the brain score in a given condition across all participants. Panel (b) depicts the Destrieux ROIs with robust loadings on the LV in panel (a) and visualised with the Freesurfer Surface (https://chrisadamsonmcri.github.io/freesurfer_statsurf_display). In the brain figure in panel (b), absolute BSR values lower than 4 have been set to zero. Panels (c) and (d) depict the brain-relevant GO enrichment terms, which are associated with upregulated genes likely to impact the Time 1 (panel c) and Time 2 (panel d) ELA/Psychopathology brain profile (i.e., PLS-derived brain LV) (panel a). ELA = early life adversity. LV = latent variable. GO = gene ontology. WM = white matter.

psychopathology-linked brain LV (i.e., ROI-specific weights) and gene expression in each of the 72 left hemisphere ROIs from the Destrieux ROIs. There emerged one gene expression profile which was significantly linked to the neurodevelopmental patterns associated with baseline ELA and Time 1/Time 2 psychopathology ($r = 0.50$, 95% CI = [.50;0.67], permutation-based $p = 0.012$). The transcriptional signature relevant to greater Time 1 $BOLD_{SV}$ in response to threat and greater LD/RD at both time points was enriched in genes relevant to anatomical structure development ($p = 4 \times 10^{-8}$), axonal ensheathment ($p = 6 \times 10^{-8}$), myelination ($p = 2 \times 10^{-7}$), angiogenesis ($p = 4 \times 10^{-8}$), cell differentiation ($p = 8 \times 10^{-6}$) and regulation of intracellular signal transduction ($p = 5 \times 10^{-6}$). Complementarily, the transcriptional profile linked to dampened RS $BOLD_{SV}$ at Time 2 was enriched in genes relevant to respiratory electron transport chain ($p = 10^{-15}$), mitochondria-related processes (*ps* from 10^{-12} to 10^{-6}), generation of precursor metabolites and energy ($p = 10^{-11}$), and cellular nitrogen compound biosynthetic process ($p = 10^{-6}$) (see Fig. 5-c, d for word clouds representing the biological processes most associated with these transcriptional profiles, as well as Supplemental Materials for a complete list of GO terms).

2.2.2.2. Accelerated biological aging and departures from typical neurodevelopmental patterns are independent mediators of ELA effects on averaged Time 1/Time 2 psychopathology risk. Finally, we turned to our core question of whether (earlier) pubertal timing and departures from typical neurodevelopmental patterns mediated the impact of baseline ELA on persistent psychopathology risk. Consistent with their aforementioned high correlation and similar associations with baseline ELA, the average of the CCA-derived Time 1 and Time 2 profiles was regarded as an index of persistent psychopathology (see Fig. 4-e, f).

ELA effects on developmental speed.

CCA. The results of ten discovery CCAs yielded one mode that was validated across all test folds ($r_{discovery}$ from.15 to.16, all *ps* $= 10^{-5}$, r_{test} =0.09, $p = 0.0001$, see Fig. 6). This mode indicated that the Time 1 ELA/averaged cross-temporal psychopathology profile was associated with reduced Time 2 resting state (RS), but heightened Time 1 threat-evoked BOLDsv, as well as delayed sensory/perceptual (SM-M, VIS), but accelerated control (FPC, SAL), memory (RSP), external attention (VAN), environmental vigilance (CON, CP), and auditory network segregation (see Fig. 6-a).

Mediation analysis. To probe the mediating role of pubertal timing and alterations in typical neurodevelopment, we specified the path model depicted in Fig. 7 as the statistical equivalent of the conceptual model depicted in Fig. 1(i.e., Hayes' Model 6). To account for the effect of Time 2 ELAs, the corresponding family conflict, neighbourhood crime and perceived parental inattentiveness scores were regressed out from the average psychopathology profile score.

The results of this analysis did not support our predicted serial mediation model (cf. Fig. 1), but instead provided evidence for parallel mediation of Time 1 ELA on persistent psychopathology via pubertal timing, $IE_1 = 0.007$, $SE = 0.003$, 95% CI = [0.001;0.014] and departure from typical neurodevelopmental patterns, $IE_2 = 0.005$, $SE = 0.003$, 95% CI = [.0004;0.010] (see Fig. 7). Of note, the two indirect effects were not statistically different from one another, $C1$ ($IE_1 - IE_2$) = 0.002, $SE = 0.004$, 95% CI = [−0.006;0.010]. However, both mediational pathways were significantly stronger than our hypothesised serial mediation path, $C2$ ($IE_1 - IE_3$) = 0.007, $SE = 0.003$, 95% CI = [0.001;0.014] (pubertal timing indirect effect) and $C3$ (IE_2–IE_3) = 0.005, $SE = 0.003$, 95% CI = [0.0004;0.011] (indirect effect of neurodevelopment). Finally, there was also evidence of a direct effect of Time 1 ELA on persistent psychopathology risk, $DE = 0.144$, $SE = 0.031$, 95% CI = [.083;0.204], which was left unexplained by the variables herein scrutinised.

3. Discussion

Extending prior reports on the distinguishable effects of threat- versus deprivation-based ELAs on biological aging and neurostructural maturation (Colich et al., 2020a, 2020b), we provide novel evidence on the strong impact of family conflict, a proximal and (typically) enduring social interaction-based form of threat (Chen et al., 2017), on pubertal timing and functional brain development. Specifically, we demonstrate that psychopathology risk linked primarily to high conflict family environments is independently associated with earlier pubertal onset and functional neurodevelopmental alterations most relevant to threat and cognitive control/attentional processes. Although driven by family conflict, the aforementioned pattern was compounded by the presence of material deprivation. As such, it was consonant with theoretical models (Cummings and Miller-Graff, 2015; McLaughlin & Sheridan, 2016) and previous reports linking more distal material hardship indicators (e.g., neighbourhood-related) to both poorer neurocognitive functioning and accelerated development of threat-relevant fronto-limbic connectivity patterns (Ramphal et al., 2020; Vargas et al., 2020).

3.1. Concurrent correlates of social threat ELAs

Recent investigations underscore the distinct (social) threat-related sequelae on neurostructural systems underpinning environmental salience processing (Colich et al., 2020a, 2020b; Miskolczi et al., 2019; Thijssen et al., 2020; Tyborowska et al., 2018). Accordingly, we report a

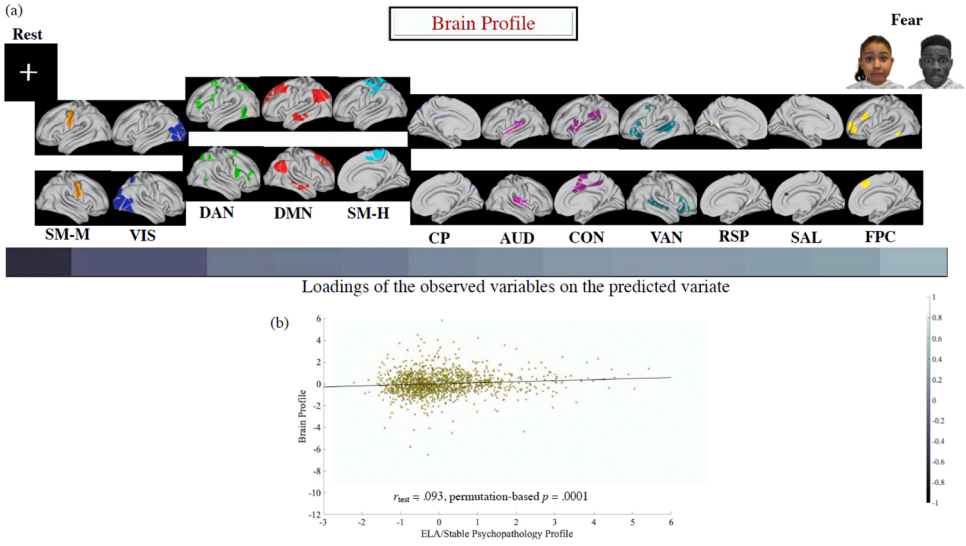

Fig. 6. The relationship of baseline ELA and psychopathology with the profile of functional neurodevelopmental alterations. The left-to-right organisation of the brain variables in panel (a) reflects the magnitude of their loading on the CCA brain variate (i.e., "Brain Profile") from the variable with the highest absolute value negative loading ("Rest") to the variable with the highest absolute value positive loading ("Fear"). The scatter plot in panel (b) describes the linear relationship between the predicted values of the two variates (i.e., Brain Profile and ELA/Psychopathology Profile) across all test CCAs. The networks in panel (a) have been visualised with the Connectome Workbench (https://www.humanconnectome.org/software/connectome-workbench). ELA = early life adversity.

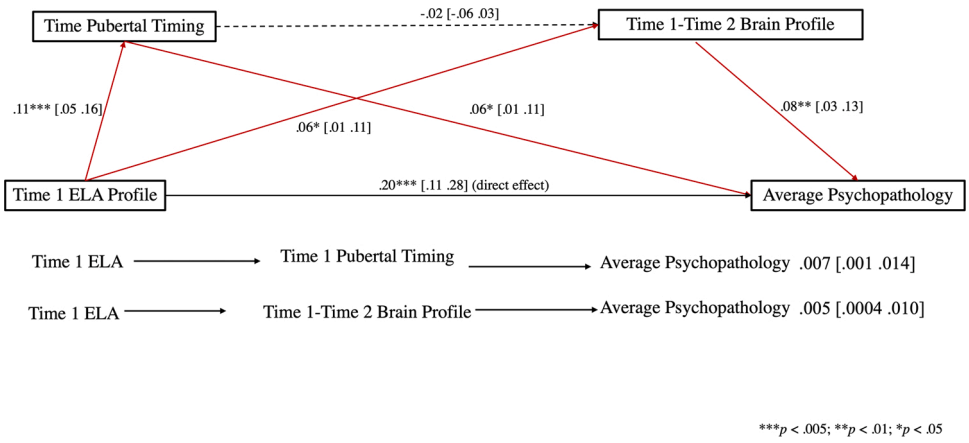

Fig. 7. Mediational model linking baseline ELA to average Time 1/Time 2 psychopathology via pubertal timing and neurodevelopmental alterations. ELA = early life adversity.

link between ongoing exposure to family conflict and greater brain-wide $BOLD_{SV}$ in response to fearful faces at Time 1, suggestive of accelerated development of threat processing systems. However, unlike studies documenting the protective role of accelerated frontolimbic development in response to threat exposure (Chahal et al., 2021; Miller et al., 2020), we find that our observed ELA-linked brain profile is a risk factor for psychopathology. The divergence in findings may reflect methodological differences in how functional neurodevelopment was operationalized. Relatedly, the two operationalizations (i.e., connectivity- vs $BOLD_{sv}$-based) could capture distinct aspects of threat processing varying in their adaptiveness (cf. Mirman et al., 2021; Suzuki et al., 2015). Alternatively/additionally, the protective role of accelerated neurodevelopment may hinge on multilevel interactions among functional and structural brain factors. Indeed, the transcriptional signature associated with the ELA brain profile at Time 1 was enriched in myelination, axonal development and angiogenesis genes. Thus, explicit modelling of cardiovascular variables coupled with use of higher regional specificity WM microstructure indices and a wider range of functional measures may be critical to understanding the conditions under which accelerated maturation may be beneficial versus detrimental (Bechler et al., 2018; Millán et al., 2018).

3.2. Delayed consequences of social threat ELAs

3.2.1. $BOLD_{sv}$. Extant literature underscores the distinguishable immediate versus delayed sequelae of ELA (Graham et al., 2021). For instance, studies of prenatal adversity effects on early postnatal development suggest that ELA-linked departures from typical development may be best captured by alternating patterns of delayed and accelerated maturation, some of which may constitute adaptive responses to the immediate environmental challenges (Ramirez et al., 2020; Rasmussen et al., 2019). Similarly, comparisons of very early life and concurrent social threat-based ELAs in adolescence highlight their opposing effects on structural neurodevelopmental pace (i.e., accelerated vs delayed, Tyborowska et al., 2018). Accordingly, we found that high family conflict exposure was linked to concurrent markers of accelerated threat processing maturation (i.e., greater threat-evoked $BOLD_{SV}$ at Time 1), but longer term indices of delayed functional neurodevelopment reflected in dampened brain-wide RS $BOLD_{sv}$ at Time 2. RS $BOLD_{sv}$ profiles have been linked to optimal neurocognitive resource allocation during task performance and flexible engagement with the external perceptual environment (Fox et al., 2007; Mennes et al., 2011; Zou et al., 2013). These findings thus imply that social threat-based ELAs may incur a pattern of concurrent affective, but protracted cognitive neurodevelopmental alterations. This reasoning is compatible with the transcriptional signature of the Time 2 ELA-linked neurodevelopmental profile, which was enriched in dopamine and attentional disorders-relevant genes (cellular nitrogen compound biosynthetic process, Thapar et al., 2016).

3.2.2. Functional network segregation. Consistent with prior investigations assessing income-based ELAs in adolescence and adulthood (Chan et al., 2018; Tooley et al., 2020), family conflict-linked psychopathology risk was associated with accelerated functional segregation of networks with protracted development, which are most vulnerable to the premature closure of neural plasticity windows triggered by ELA (Callaghan and Tottenham, 2016; Grayson and Fair, 2017; Miskolczi et al., 2019). Thus, most affected were networks relevant to cognitive control (FPC), environmental vigilance and adaptability (CON, SAL), navigational and episodic memory (RSP) and external attention processes (VAN) (Corbetta & Shulman, 2002; Dosenbach et al., 2007; Duncan et al., 2020; Murray et al., 2017). While ELA-triggered closure of neural plasticity windows has been linked to earlier pubertal hormone rise (Laube et al., 2020), in our study, pubertal timing and neurodevelopmental alterations independently mediated the impact of ELA on psychopathology, implying that distinct mechanisms could be at play. Thus, finer tuned investigations explicitly modelling the impact of pubertal hormone levels on functional and structural neurodevelopment are certainly warranted.

More broadly, because our ELA measures assessed relatively stable environmental characteristics, our documented effect of family conflict on accelerated functional network segregation is compatible with recent neurodevelopmental models that posit a link between repetitive negative experiences and accelerated functional specialisation (i.e., earlier declining neural plasticity) (Tooley et al., 2021). Such associations presumably reflect the increase in glucocorticoid levels and inflammatory processes evoked by chronic adverse experiences, which unleash global aging processes. Expanding this reasoning, our results imply that it is enduring, immediate (i.e, close social interaction-based) negative experiences that impact allostatic load the most (Cummings & Miller-Graf, 2015).

It is worth pointing out that ELA/Psychopathology profiles were most strongly linked to functional neurodevelopment rate, thereby raising the possibility that they indirectly reduced the coupling of structural and functional development herein documented. Previous reports underscored the beneficial effects of coupled developmental changes in structure and function, particularly for brain regions relevant to cognitive control functions (Baum et al., 2020). Consequently, a question for future research is to elucidate the relative contribution of accelerated/delayed functional maturation versus uncoupling of structural-functional development to the adverse effects of ELA, as well as uncover their potentially dissociable transcriptional signatures.

3.3. Typical profiles of functional and structural neurodevelopment

To our knowledge, only a handful of studies documented a robust link between BOLDsv and WM microstructure (Burzynska et al., 2015; Easson and McIntosh, 2019; Wang et al., 2021). Extending this research, we provide regionally specific evidence that maturational increases in FA are associated with corresponding widespread RS and task-related increases (rest, cf. Easson & McIntosh, 2019), but also task-related decreases in $BOLD_{sv}$, particularly in areas linked to externally oriented processing (Garrett et al., 2020; Grady and Garrett, 2018). Our investigation thus extends prior evidence of developmental increments in FA, presumably indicative of greater refinement in axonal structure and higher myelination (Vettel et al., 2017; Lebel and Deoni, 2018), by demonstrating that such structural changes supportive of increasingly directional neuronal communication accompany increasingly robust mental process-specific neural responses. Furthermore, we show that this rising functional specialisation is yoked to increments in intrinsic (task-free) functional network segregation, consistent with the argument that the latter reflects a history of task-related co-activation (Gabard-Durnam et al., 2016; Geng et al., 2021; Wig et al., 2011). Complementarily, regionally specific developmental decrements in FA, potentially suggestive of less directionally coherent and more complex fibre configurations (Huber et al., 2019) are associated with maturational increases in BOLDsv during task, possibility indicative of more flexible responses to the environment. Accordingly, we show that these yoked changes in BOLD signal stabilisation and WM microstructure are associated with transcriptional profiles enriched in genes relevant to synaptic processes, responses to the external environment and anatomical structure morphogenesis.

3.4. Limitations and future directions

First, we only had access to data from two time points. Multiple data waves would facilitate implementation of more stringent mediation analyses that could avoid the methodological and interpretive difficulties associated with concurrent predictor and mediator variables (Bullock et al., 2010). They would also allow use of growth curve analysis to characterise both homogenous and heterogenous neural and pubertal developmental trajectories, potentially, unveiling intricate patterns of ELA-induced maturational slowdown and acceleration (Becht and Mills, 2020; Mills et al., 2021; Ramirez et al., 2020; Rasmussen et al., 2019). Access to multiple data points would thus enable more in-depth investigation of the quantitatively modest, yet robust (see Fig. S5) neural mediational pathway herein documented, which could have substantive implications for identifying at-risk individuals (see Kelley and Preacher, 2012, for a discussion of quantitative versus pragmatically relevant effect sizes, as well as Preacher and Kelley, 2011, for difficulties in deciding on an effect size threshold for mediation analyses). Second, we used only parent reports of youth psychopathology because clinical evaluation of youth experiences showed limited variability and substantial missing data. Thus, future research incorporating data from additional raters (e.g., youth, peers, teachers) and modalities (e.g., behavioural observation, diary) would shed further light on the effects herein documented. Third, future studies assessing a wider range of threats (beyond family conflict and neighbourhood crime) are needed to elucidate the shared and unique mechanisms through which different forms of violence impact neurodevelopment. Fourth, sampling of a wider task range, including naturalistic paradigms (e.g., movie watching), and use of multiple brain atlases and techniques to estimate functional and structural connectivity (Bijsterbosch et al., 2020; Edwards et al., 2017; Eickhoff et al., 2018) would provide important insights into the boundary conditions of the effects herein reported. Fifth, future investigations combining hormonal measures with self, parental or physician indices of pubertal development (e.g., Herting et al., 2021) could determine the mechanisms underlying the impact of ELA on pubertal and brain development. Sixth, our focus on coupled structural-functional developmental alterations led to the elimination of participants with poor quality data in any of the scrutinitised modalities, and, thus, unfortunately, a reduction in the racial/ethnic diversity of the ABCD sample. Although we verified that our ELA-psychopathology findings were replicated in these eliminated participants (Fig. S6), it is possible that our present findings are most relevant to Caucasian individuals (see Simons et al., 2017 for a discussion of the inherent constraints to generality associated with any research). Further investigation is thus needed into potential links between participants' neuroimaging data quality and sociodemographic variables, including racial/ethinic background and ELA. Seventh, we used gene expression data from six postmortem adult brains (mean age = 43 years) provided by the Allen Institute of Brain Science because, to our knowledge, this constituted the most comprehensive resource available. The same approach and gene dataset have been used before to investigate the transcriptional profiles associated with adolescent structural neurodevelopment (Ball et al., 2020; Park et al., 2021; Whitaker et al., 2016). This approach is defensible because most age-related transcriptional differences reportedly occur in the prenatal to infancy/early childhood period (~up to 6 years of age) (Kang et al., 2011). Furthermore, any such differences would have likely hindered our ability to find meaningful associations between the neuroimaging and gene expression data. Nonetheless, availability of comprehensive transcriptomic datasets covering childhood and adolescence would increase the sensitivity of neuroimaging-transcriptomics associations. Eighth, genetic susceptibility to earlier maturation moderates the impact of ELA on biological aging (Sun et al., 2020). Relatedly, biological aging rate, as indexed by pubertal timing, varies across different racial groups. Moreover, for children living with their biological parents, shared genetic influences may inflate estimates of family environment effects (Harold and Sellers, 2018; Harold et al., 2013; Horwitz et al., 2010). Thus, future studies using polygenic risk measures of developmental pace in ethnically/racially diverse samples of biological and adoptive families, potentially, within a twin design, could characterise gene-environment interactions that modulate the impact of ELA.

4. Conclusions

Our results underscore the potent contribution of family conflict to concurrent and temporally distal pychopathology (i.e., behavioural dysregulation, attentional problems). Importantly, they also suggest that these ELA-psychopathology links are mediated by parallel mechanisms involving earlier pubertal maturation and a mix of accelerated and delayed functional neurodevelopmental patterns. Given that accelerated brain aging is a key marker of adult psychopathology (e.g., Kuo et al., 2020), a priority for future longitudinal studies would be to characterise the link between developmental/aging speed and psychopathology across various ELAs and life stages.

Data statement

The raw data are available at https://nda.nih.gov/abcd upon completion of the relevant data use agreements. The ABCD data repository grows and changes over time. The ABCD data used in this report came from Adolescent Brain Cognitive Development Study (ABCD) - Annual Release 3.0 #901. DOIs can be found at https://doi.org/10.15154/1519007.

Conflict of interest

The authors declare no competing interests.

Data availability

We used already existing code, as specified in the main text with links for free download.

Acknowledgements

Data used in the preparation of this article were obtained from the Adolescent Brain Cognitive Development (ABCD) Study (https://abcdstudy.org), held in the NIMH Data Archive (NDA). This is a multi-site, longitudinal study designed to recruit more than 10,000 children age 9–10 and follow them over 10 years into early adulthood. The ABCD Study is supported by the National Institutes of Health and additional federal partners under award numbers U01DA041048, U01DA050989, U01DA051016, U01DA041022, U01DA051018, U01DA051037, U01DA050987, U01DA041174, U01DA041106, U01DA041117, U01DA041028, U01DA041134, U01DA050988, U01DA051039, U01DA041156, U01DA041025, U01DA041120, U01DA051038, U01DA041148, U01DA041093, U01DA041089, U24DA041123, U24DA041147. A full list of supporters is available at https://abcdstudy.org/federal-partners.html. A listing of participating sites and a complete listing of the study investigators can be found at https://abcdstudy.org/consortium_members/. ABCD consortium investigators designed and implemented the study and/or provided data but did not necessarily participate in analysis or writing of this report. This manuscript reflects the views of the authors and may not reflect the opinions or views of the NIH or ABCD consortium investigators. The work was partially supported by a grant from the Waterloo Foundation

Appendix A. Supporting information

Supplementary data associated with this article can be found in the online version at doi:10.1016/j.dcn.2021.101032.

References

Achenbach, T.M., 2009. The Achenbach System of Empirically Based Assessment (ASEBA): Development, Findings, Theory and Applications. University of Vermont Research Center for Children, Youth and Families, Burlington, VT.

Andersson, J.L., Skare, S., Ashburner, J., 2003. How to correct susceptibility distortions in spin-echo echo-planar images: application to diffusion tensor imaging. NeuroImage 20, 870–888.

Arnatkevičiūtė, A., Fulcher, B.D., Fornito, A., 2019. A practical guide to linking brain-wide gene expression and neuroimaging data. NeuroImage 189, 353–367.

Ball, G., Seidlitz, J., Beare, R., Seal, M.L., 2020. Cortical remodelling in childhood is associated with genes enriched for neurodevelopmental disorders. NeuroImage 215, 116803.

Banihashemi, L., Peng, C.W., Verstynen, T., Wallace, M.L., Lamont, D.N., Alkhars, H.M., Yeh, F.C., Beeney, J.E., Aizenstein, H.J., Germain, A., 2021. Opposing relationships of childhood threat and deprivation with stria terminalis white matter. Hum. Brain Mapp. 42, 2445–2460.

Baracchini, G., Mišić, B., Setton, R., Mwilambwe-Tshilobo, L., Girn, M., Nomi, J.S., Uddin, L.Q., Turner, G.R., Spreng, R.N., 2021. Inter-regional BOLD signal variability is an organizational feature of functional brain networks. NeuroImage 237, 118149. https://doi.org/10.1016/j.neuroimage.2021.118149.

Barch, D.M., Burgess, G.C., Harms, M.P., Petersen, S.E., Schlaggar, B.L., Corbetta, M., Glasser, M.F., Curtiss, S., Dixit, S., Feldt, C., Nolan, D., Bryant, E., Hartley, T., Footer, O., Bjork, J.M., Poldrack, R., Smith, S., Johansen-Berg, H., Snyder, A.Z., Van Essen, D.C., for the WU-Minn HCP Consortium, 2013. Function in the human connectome: Task-fMRI and individual differences in behavior. NeuroImage 80, 169–189.

Basser, P.J., Mattiello, J., LeBihan, D., 1994. MR diffusion tensor spectroscopy and imaging. Biophys. J. 66, 259–267.

Bechler, M.E., Swire, M., Ffrench-Constant, C., 2018. Intrinsic and adaptive myelination-A sequential mechanism for smart wiring in the brain. Dev. Neurobiol. 78, 68–79.

Becht, A.I., Mills, K.L., 2020. Modeling individual differences in brain development. Biol. Psychiatry 88, 63–69.

Bijsterbosch, J., Harrison, S.J., Jbabdi, S., Woolrich, M., Beckmann, C., Smith, S., Duff, E. P., 2020. Challenges and future directions for representations of functional brain organization. Nat. Neurosci. 23, 1484–1495.

Bissett, P.G., Hagen, M.P., Jones, H.M., Poldrack, R.A., 2021. Design issues and solutions for stop-signal data from the Adolescent Brain Cognitive Development (ABCD) study. eLife 10, e60185.

Bronfenbrenner, U., Evans, G.W., 2000. Developmental science in the 21st century: emerging questions, theoretical models, research designs, and empirical findings. Social Dev. 9, 115–125.

Bullock, J.G., Green, D.P., Ha, S.E., 2010. Yes, but what's the mechanism? (don't expect an easy answer). J. Pers. Social Psychol. 98, 550–558.

Burzynska, A.Z., Wong, C.N., Voss, M.W., Cooke, G.E., McAuley, E., Kramer, A.F., 2015. White matter integrity supports BOLD signal variability and cognitive performance in the aging human brain. PLoS One 10, e0120315.

Callaghan, B.L., Tottenham, N., 2016. The stress acceleration hypothesis: effects of early-life adversity on emotion circuits and behavior. Curr. Opini. Behav. Sci. 7, 76–81.

Casey, B.J., Cannonier, T., Conley, M.I., Cohen, A.O., Barch, D.M., Heitzeg, M.M., Soules, M.E., Teslovich, T., Dellarco, D.V., Garavan, H., Orr, C.A., Wager, T.D., Banich, M.T., Speer, N.K., Sutherland, M.T., Riedel, M.C., Dick, A.S., Bjork, J.M., Thomas, K.M., Chaarani, B., Mejia, M.H., Hagler Jr., D.J., Daniela Cornejo, M., Sicat, C.S., Harms, M.P., Dosenbach, N.U.F., Rosenberg, M., Earl, E., Bartsch, H., Watts, R., Polimeni, J.R., Kuperman, J.M., Fair, D.A., Dale, A.M., ABCD Imaging Acquisition Workgroup, 2018. The adolescent brain cognitive development (ABCD) study: imaging acquisition across 21 sites. Dev. Cognit. Neurosci. 32, 43–54.

Chahal, R., Kirshenbaum, J.S., Ho, T.C., Mastrovito, D., Gotlib, I.H., 2021. Greater age-related changes in white matter morphometry following early life stress: Associations with internalizing problems in adolescence. Dev. Cognit. Neurosci. 47, 100899.

Chang, L.C., Jones, D.K., Pierpaoli, C., 2005. RESTORE: robust estimation of tensors by outlier rejection. Magn. Resonance Med. 53, 1088–1095.

Chan, M.Y., Na, J., Agres, P.F., Savalia, N.K., Park, D.C., Wig, G.S., 2018. Socioeconomic status moderates age-related differences in the brain's functional network organization and anatomy across the adult lifespan. Proc. Natl. Acad. Sci. U. S. A. 115, E5144–E5153.

Chan, M., Park, D.C., Savalia, N.K., Petersen, S.E., Wig, G.S., 2014. Decreased segregation of brain systems across the healthy adult lifespan. Proc. Natl. Acad. Sci. U. S. A. 111, E4997–E5006.

Chen, E., Brody, G.H., Miller, G.E., 2017. Childhood close family relationships and health. Am. Psycholo. 72, 555–566.

Chilcoat, H.D., Anthony, J.C., 1996. Impact of parent monitoring on initiation of drug use through late childhood. J. Am. Acade. Child Adolesc. Psychiatry 35, 91–100.

Clark, L.A., Watson, D., 1995. Constructing validity: Basic issues in objective scale development. Psychol. Assess. 7, 309–319.

Colich, N.L., Platt, J.M., Keyes, K.M., Sumner, J.A., Allen, N.B., McLaughlin, K.A., 2020b. Earlier age at menarche as a transdiagnostic mechanism linking childhood trauma with multiple forms of psychopathology in adolescent girls. Psychol. Med. 50, 1090–1098.

Colich, N.L., Rosen, M.L., Williams, E.S., McLaughlin, K.A., 2020a. Biological aging in childhood and adolescence following experiences of threat and deprivation: a systematic review and meta-analysis. Psychol. Bull. 146, 721–764.

Conley, M.I., Dellarco, D.V., Rubien-Thomas, E.A., Cervera Tottenham, N., Casey, B.J., 2017. The Racially Diverse Affective Expressions (RADIATE) Face Set of Stimuli. Proceedings of the Association for Psychological Science, Boston, MA.

Corbetta, M., Shulman, G.L., 2002. Control of goal-directed and stimulus-driven attention in the brain. Nat. Rev. Neurosci. 3, 201–215.

Cox, R.W., 1996. AFNI: software for analysis and visualization of functional magnetic resonance neuroimages. Comput. Biomed. Res. 29, 162–173.

Crone, E., Dahl, R., 2012. Understanding adolescence as a period of social–affective engagement and goal flexibility. Nat. Rev. Neurosci. 13, 636–650.

Cummings, E.M., Goeke-Morey, M.C., Merrilees, C.E., Taylor, L.K., Shirlow, P., 2014. A social–ecological, process-oriented perspective on political violence and child development. Child Dev. Perspect. 8, 82–89.

Cummings, E.M., Miller-Graff, L.E., 2015. Emotional security theory: an emerging theoretical model for youths' psychological and physiological responses across multiple developmental contexts. Curr. Directions Psychol. Sci. 24, 208–213.

Dennison, M.J., Sheridan, M.A., Busso, D.S., Jenness, J.L., Peverill, M., Rosen, M.L., McLaughlin, K.A., 2016. Neurobehavioral markers of resilience to depression amongst adolescents exposed to child abuse. J. Abnorm. Psychol. 125, 1201–1212.

Destrieux, C., Fischl, B., Dale, A., Halgren, E., 2010. Automatic parcellation of human cortical gyri and sulci using standard anatomical nomenclature. Neuroimage 53, 1–15.

Diemer, M.A., Mistry, R.S., Wadsworth, M.E., Lopez, I., Reimers, F., 2012. Best practices in conceptualizing and measure social class in psychological research. Anal. Social Issues Public Policy 13, 77–113.

Dosenbach, N.U., Fair, D.A., Miezin, F.M., Cohen, A.L., Wenger, K.K., Dosenbach, R.A., Fox, M.D., Snyder, A.Z., Vincent, J.L., Raichle, M.E., Schlaggar, B.L., Petersen, S.E., 2007. Distinct brain networks for adaptive and stable task control in humans. Proc. Natl. Acad. Sci. U. S. A. 104, 11073–11078.

Easson, A.K., McIntosh, A.R., 2019. BOLD signal variability and complexity in children and adolescents with and without autism spectrum disorder. Dev. Cognit. Neurosci. 36, 100630.

Echeverria, S.E., Diez-Roux, A.V., Link, B.G., 2004. Reliability of self-reported neighborhood characteristics. J. Urban Health 81, 682–701.

Eden, E., Lipson, D., Yogev, S., Yakhini, Z., 2007. Discovering motifs in ranked lists of DNA sequences. PLoS Comput. Biol. 3 (e39), 2007.

Eden, E., Navon, R., Steinfeld, I., Lipson, D., Yakhini, Z., 2009. GOrilla: a tool for discovery and visualization of enriched GO terms in ranked gene lists. BMC Bioinf. 10, 48.

Edwards, L.J., Pine, K.J., Ellerbrock, I., Weiskopf, N., Mohammadi, S., 2017. NODDI-DTI: estimating neurite orientation and dispersion parameters from a diffusion tensor in healthy white matter. Front. Neurosci. 11, 720.

Eickhoff, S.B., Yeo, B., Genon, S., 2018. Imaging-based parcellations of the human brain. Nat. Rev. Neurosci. 19, 672–686.

Fair, D.A., Miranda-Dominguez, O., Snyder, A.Z., Perrone, A.A., Earl, E.A., Van, A.N., Koller, J.M., Feczko, E., Klein, R.L., Mirro, A.E., Hampton, J.M., Adeyemo, B., Laumann, T.O., Gratton, C., Greene, D.J., Schlaggar, B., Hagler, D., Watts, R., Garavan, H., Barch, D.M., Nigg, J.T., Petersen, S.E., Dale, A., Feldstein-Ewing, S.W., Nagel, B.J., Dosenbach, N.U.F., 2020. Correction of respiratory artifacts in MRI head motion estimates. NeuroImage 208, 116400.

Fischl, B., Salat, D.H., Busa, E., Albert, M., Dieterich, M., Haselgrove, C., van der Kouwe, A., Killiany, R., Kennedy, D., Klaveness, S., Montillo, A., Makris, N., Rosen, B., Dale, A.M., 2002. Whole brain segmentation: automated labeling of neuroanatomical structures in the human brain. Neuron 33, 341–355.

Fox, M.D., Snyder, A.Z., Vincent, J.L., Raichle, M.E., 2007. Intrinsic fluctuations within cortical systems account for intertrial variability in human behavior. Neuron 56, 171–184.

Fulcher, B.D., Little, M.A., Jones, N.S., 2013. Highly comparative time-series analysis: the empirical structure of time series and their methods. J. R. Soc. Interface 10, 20130048.

Funkhouser, C.J., Chacko, A.A., Correa, K.A., Kaiser, A.J.E., Shankman, S.A., 2021. Unique longitudinal relationships between symptoms of psychopathology in youth: a cross-lagged panel network analysis in the ABCD study. J. Child Psychol. Psychiatry Allied Discip. 62, 184–194.

Gabard-Durnam, L.J., Gee, D.G., Goff, B., Flannery, J., Telzer, E., Humphreys, K.L., Lumian, D.S., Fareri, D.S., Caldera, C., Tottenham, N., 2016. Stimulus-elicited connectivity influences resting-state connectivity years later in human development: a prospective study. J. Neurosci. 36, 4771–4784.

Garavan, H., Chaarani, B., Hahn, S., Allgaier, N., Juliano, A., Yuan, D.K., Orr, C., Watts, R., Wager, T.D., Ruiz de Leon, O., Hagler Jr, D.J. & Potter, A., 2021, The ABCD Stop Signal Data: Response to Bissett et al. https://www.biorxiv.org/content/10.1101/2020.07.27.223057v2.

Garrett, D.D., Epp, S.M., Kleemeyer, M., Lindenberger, U., Polk, T.A., 2020. Higher performing older adults upregulate brain signal variability in response to feature-rich sensory input. NeuroImage 217, 116836.

Gehred, M.Z., Knodt, A.R., Ambler, A., Bourassa, K.J., Danese, A., Elliott, M.L., Hogan, S., Ireland, D., Poulton, R., Ramrakha, S., Reuben, A., Sison, M.L., Moffitt, T.E., Hariri, A.R., Caspi, A., 2021. Long-term Neural Embedding of Childhood Adversity in a Population-Representative Birth Cohort Followed for 5 Decades. Biol. psychiatry 90, 182–193.

Geng, F., Botdorf, M., Riggins, T., 2021. How behavior shapes the brain and the brain shapes behavior: Insights from memory development. J. Neurosci. 41, 981–990.

Gordon, E.M., Laumann, T.O., Adeyemo, B., Huckins, J.F., Kelley, W.M., Petersen, S.E., 2016. Generation and evaluation of a cortical area parcellation from resting-state correlations. Cerebral Cortex 26, 288–303.

Grady, C.L., Garrett, D.D., 2018. Brain signal variability is modulated as a function of internal and external demand in younger and older adults. NeuroImage 169, 510–523.

Graham, A.M., Marr, M., Buss, C., Sullivan, E.L., Fair, D.A., 2021. Understanding vulnerability and adaptation in early brain development using network neuroscience. Trends Neurosci. 44, 276–288. https://doi.org/10.1016/j.tins.2021.01.008.

Grahek, I., Shenhav, A., Musslick, S., Krebs, R.M., Koster, E.H., 2019. Motivation and cognitive control in depression. Neurosci. Biobehav. Rev. 102, 371–381.

Grayson, D.S., Fair, D.A., 2017. Development of large-scale functional networks from birth to adulthood: a guide to the neuroimaging literature. NeuroImage 160, 15–31.

Hagler Jr., D.J., Ahmadi, M.E., Kuperman, J., Holland, D., McDonald, C.R., Halgren, E., Dale, A.M., 2009. Automated white-matter tractography using a probabilistic diffusion tensor atlas: application to temporal lobe epilepsy. Hum. Brain Mapp. 30, 1535–1547.

Hagler DJ, Jr, Hatton, S., Cornejo, M.D., Makowski, C., Fair, D.A., Dick, A.S., Sutherland, M.T., Casey, B.J., Barch, D.M., Harms, M.P., Watts, R., Bjork, J.M., Garavan, H.P., Hilmer, L., Pung, C.J., Sicat, C.S., Kuperman, J., Bartsch, H., Xue, F., Heitzeg, M.M., Laird, A.R., Trinh, T.T., Gonzalez, R., Tapert, S.F., Riedel, M.C., Squeglia, L.M., Hyde, L.W., Rosenberg, M.D., Earl, E.A., Howlett, K.D., Baker, F.C., Soules, M., Diaz, J., de Leon, O.R., Thompson, W.K., Neale, M.C., Herting, M., Sowell, E.R., Alvarez, R.P., Hawes, S.W., Sanchez, W.K., Bodurka, J., Breslin, F.J., Morris, A.S., Paulus, M.P., Simmons, W.K., Polimeni, J.R., van der Kouwe, A., Nencka, A.S., Gray, K.M., Pierpaoli, C., Matochik, J.A., Noronha, A., Aklin, W.M., Conway, K., Glantz, M., Hoffman, E., Little, R., Lopez, M., Barch, V., Weiss, S.R., Wolff-Hughes, D.L., DelCarmen-Wiggins, R., Feldstein Ewing, S.W., Miranda-Dominguez, O., Nagel, B.J., Perrone, A.J., Sturgeon, D.T., Goldstone, A., Pfefferbaum, A., Pohl, K.M., Prouty, D., Uban, K., Bookheimer, S.Y., Dapretto, M., Galvan, A., Bagot, K., Giedd, J., Infante, M.A., Jacobus, J., Patrick, K., Shilling, P.D., Desikan, R., Li, Y., Sugrue, L., Banich, M.T., Friedman, N., Hewitt, J.K., Hopfer, C., Sakai, J., Tanabe, J., Cottler, L.B., Nixon, S.J., Chang, L., Cloak, C., Nagel, T., Reeves, G., Kennedy, D.N., Heeringa, S., Peltier, S., Schulenberg, J., Sripada, C., Zucker, R.A., Iacono, W.G., Luciana, M., Calabro, F.J., Clark, D.B., Lewis, D.A., Luna, B., Schirda, C., Brima, T., Foxe, J.J., Freedman, E.G., Mruzek, D.W., Mason, M.J., Huber, R., McGlade, E., Prescot, A., Renshaw, P.F., Yurgelun-Todd, D.A., Allgaier, N.A., Dumas, J.A., Ivanova, M., Potter, A., Florsheim, P., Larson, C., Lisdahl, K., Charness, M.E., Fuemmeler, B., Hettema, J.M., Maes, H.H., Florsheim, J., Anokhin, A.P., Glaser, P., Heath, A.C., Madden, P.A., Baskin-Sommers, A., Constable, R.T., Grant, S.J., Dowling, G.J., Brown, S.A., Jernigan, T.L., Dale, A.M., 2019. Image processing and analysis methods for the Adolescent Brain Cognitive Development Study. NeuroImage 202, 116091.

Hair, J.F., Tatham, R.L., Anderson, R.E., Black, W., 1998. Multivariate Data Analysis. Prentice-Hall, London.

Hansen, J.Y., Markello, R.D., Vogel, J.W., Seidlitz, J., Bzdok, D., Misic, B., 2021. Mapping gene transcription and neurocognition across human neocortex. Nat. Hum. Behav. 5, 1240–1250. https://doi.org/10.1038/s41562-021-01082-z.

Hanson, J.L., Hariri, A.R., Williamson, D.E., 2015. Blunted ventral striatum development in adolescence reflects emotional neglect and predicts depressive symptoms. Biol. Psychiatry 78, 598–605.

Hanson, J.L., van den Bos, W., Roeber, B.J., Rudolph, K.D., Davidson, R.J., Pollak, S.D., 2017. Early adversity and learning: implications for typical and atypical behavioral development. J. Child Psychol. Psychiatry, Allied Discip. 58, 770–778.

Harold, G.T., Leve, L.D., Elam, K.K., Thapar, A., Neiderhiser, J.M., Natsuaki, M.N., Shaw, D.S., Reiss, D., 2013. The nature of nurture: disentangling passive genotype-environment correlation from family relationship influences on children's externalizing problems. J. Family Psychol. 27, 12–21.

Harold, G.T., Sellers, R., 2018. Annual Research Review: interparental conflict and youth psychopathology: an evidence review and practice focused update. J. Child Psychol. Psychiatry, Allied Discip. 59, 374–402.

Hawrylycz, M., Miller, J.A., Menon, V., Feng, D., Dolbeare, T., Guillozet-Bongaarts, A.L., Jegga, A.G., Aronow, B.J., Lee, C.K., Bernard, A., Glasser, M.F., Dierker, D.L., Menche, J., Szafer, A., Collman, F., Grange, P., Berman, K.A., Mihalas, S., Yao, Z., Stewart, L., Barabási, A.L., Schulkin, J., Phillips, J., Ng, L., Dang, C., Haynor, D.R., Jones, A., Van Essen, D.C., Koch, C., Lein, E., 2015. Canonical genetic signatures of the adult human brain. Nat. Neurosci. 18, 1832–1844.

Hayes, A., Cai, L., 2007. Using heteroskedasticity-consistent standard error estimators in OLS regression: an introduction and software implementation. Behav. Res. Methods 39, 709–722.

Hayes, A.F., Scharkow, M., 2013. The relative trustworthiness of inferential tests of the indirect effect in statistical mediation analysis: does method really matter? Psychol. Sci. 10, 1918–1927.

Hayes, A.F., 2018. Introduction to Mediation, Moderation, and Conditional Process Analysis: A Regression-Based Approach, Second edition.,. Guilford Press, New York.

Herting, M.M., Uban, K.A., Gonzalez, M.R., Baker, F.C., Kan, E.C., Thompson, W.K., Granger, D.A., Albaugh, M.D., Anokhin, A.P., Bagot, K.S., Banich, M.T., Barch, D.M., Baskin-Sommers, A., Breslin, F.J., Casey, B.J., Chaarani, B., Chang, L., Clark, D.B., Cloak, C.C., Constable, R.T., Cottler, L.B., Dagher, R.K., Dapretto, M., Dick, A.S., Dosenbach, N., Dowling, G.J., Dumas, J.A., Edwards, S., Ernst, T., Fair, D.A., Feldstein-Ewing, S.W., Freedman, E.G., Fuemmeler, B.F., Garavan, H., Gee, D.G., Giedd, J.N., Glaser, P., Goldstone, A., Gray, K.M., Hawes, S.W., Heath, A.C., Heitzeg, M.M., Hewitt, J.K., Heyser, C.J., Hoffman, E.A., Huber, R.S., Huestis, M.A., Hyde, L.W., Infante, M.A., Ivanova, M.Y., Jacobus, J., Jernigan, T.L., Karcher, N.R., Laird, A.R., LeBlanc, K.H., Lisdahl, K., Luciana, M., Luna, B., Maes, H.H., Marshall, A.T., Mason, M.J., McGlade, E.C., Morris, A.S., Nagel, B.J., Neigh, G.N., Palmer, C.E., Paulus, M.P., Potter, A.S., Puttler, L.I., Rajapakse, N., Rapuano, K., Reeves, G., Renshaw, P.F., Schirda, C., Sher, K.J., Sheth, C., Shilling, P.D., Squeglia, L.M., Sutherland, M.T., Tapert, S.F., Tomko, R.L., Yurgelun-Todd, D., Wade, N.E., Weiss, S., Zucker, R.A., Sowell, E.R., 2021. Correspondence between perceived pubertal development and hormone levels in 9-10 year-olds from the adolescent brain cognitive development study. Front. Endocrinol. 11, 549928.

Horwitz, B.N., Neiderhiser, J.M., Ganiban, J.M., Spotts, E.L., Lichtenstein, P., Reiss, D., 2010. Genetic and environmental influences on global family conflict. J. Family Psychol. 24, 217–220.

Hotelling, H., 1936. Relations between two sets of variables. Biometrika 28, 321–377.

Huber, E., Henriques, R.N., Owen, J.P., Rokem, A., Yeatman, J.D., 2019. Applying microstructural models to understand the role of white matter in cognitive development. Dev. Cognit. Neurosci. 36, 100624.

Ironside, M., Kumar, P., Kang, M.-S., Pizzagalli, D.E., 2018. Brain mechanisms mediating effects of stress on reward sensitivity. Curr. Opin. Behav. Sci. 22, 106–113.

Jia, T., Ing, A., Quinlan, E.B., Tay, N., Luo, Q., Francesca, B., Banaschewski, T., Barker, G.J., Bokde, A., Bromberg, U., Büchel, C., Desrivières, S., Feng, J., Flor, H., Grigis, A., Garavan, H., Gowland, P., Heinz, A., Ittermann, B., Martinot, J.L., Martinot, M.P., Nees, F., Orfanos, D.P., Paus, T., Poustka, L., Fröhner, J.H., Smolka, M.N., Walter, H., Whelan, R., Schumann, G., IMAGEN, C., 2020. Neurobehavioural characterisation and stratification of reinforcement-related behaviour. Nat. Hum. Behav. 4, 544–558.

Johnson, A., Bathelt, J., Akarca, D., Crickmore, G., Astle, D.E., 2021. Far and wide: associations between childhood socio-economic status and brain connectomics. Dev. Cognit. Neurosci. 48, 100888.

Jovicich, J., Czanner, S., Greve, D., Haley, E., van der Kouwe, A., Gollub, R., Kennedy, D., Schmitt, F., Brown, G., Macfall, J., Fischl, B., Dale, A., 2006. Reliability in multi-site structural MRI studies: effects of gradient non-linearity correction on phantom and human data. Neuroimage 30, 436–443.

Juraska, J.M., Willing, J., 2017. Pubertal onset as a critical transition for neural development and cognition. Brain Res. 1654 (Pt B), 87–94.

Kang, H.J., Kawasawa, Y.I., Cheng, F., Zhu, Y., Xu, X., Li, M., Sousa, A.M., Pletikos, M., Meyer, K.A., Sedmak, G., Guennel, T., Shin, Y., Johnson, M.B., Krsnik, Z., Mayer, S., Fertuzinhos, S., Umlauf, S., Lisgo, S.N., Vortmeyer, A., Weinberger, D.R., Mane, S., Hyde, T.M., Huttner, A., Reimers, M., Kleinman, J.E., Sestan, N., 2011. Spatio-temporal transcriptome of the human brain. Nature 478 (7370), 483–489.

Kanwisher, N., 2001. Neural events and perceptual awareness. Cognition 79, 89–113.

Kasparek, S.W., Jenness, J.L., McLaughlin, K.A., 2020. Reward processing modulates the association between trauma exposure and externalizing psychopathology. Clin. Psychol. Sci. 8, 989–1006.

Kelley, K., Preacher, K.J., 2012. On effect size. Psycholo. Methods 17, 137–152.

Knutson, B., Westdorp, A., Kaiser, E., Hommer, D., 2000. FMRI visualization of brain activity during a monetary incentive delay task. Neuroimage 12, 20–27.

Krishnan, A., Williams, L.J., McIntosh, A.R., Abdi, H., 2011. Partial Least Squares (PLS) methods for neuroimaging: a tutorial andreview. NeuroImage 56, 455–475.

Kuo, C.-Y., Lee, P.-L., Hung, S.-C., Liu, L.-K., Lee, Wei-Ju, Chung, C.-P., Yang, A.C., Tsai, S.-J., Wang, P.-N., Chen, L.-K., Chou, K.-H., Lin, C.-P., 2020. Large-scale structural covariance networks predict age in middle-to-late adulthood: a novel brain aging biomarker. Cerebral Cortex 30, 5844–5862.

Laube, C., van den Bos, W., Fandakova, Y., 2020. The relationship between pubertal hormones and experience-dependent plasticity: Implications for cognitive training in adolescence. Dev. Cognit. Neurosci. 42, 100753.

Lebel, C., Deoni, S., 2018. The development of brain white matter microstructure. Neuroimage 182, 207–218.
Leemans, A., Jones, D.K., 2009. The B-matrix must be rotated when correcting for subject motion in DTI data. Magn. Resonance Med. 61, 1336–1349.
Logan, G.D., 1994. On the ability to inhibit thought and action: a users' guide to the stop signal paradigm. In: Dagenbach, D., Carr, T.H. (Eds.), Inhibitory Processes in Attention, Memory, and Language. Academic Press, San Diego, pp. 189–239.
Lopez, M., Ruiz, M.O., Rovnaghi, C.R., Tam, G.K., Hiscox, J., Gotlib, I.H., Barr, D.A., Carrion, V.G., Anand, K.J., 2021. The social ecology of childhood and early life adversity. Pediatr. Res. 89, 353–367.
Marshall, W.A., Tanner, J.M., 1969. Variations in pattern of pubertal changes in girls. Arch. Dis. Childhood 44, 291–303.
Marshall, W.A., Tanner, J.M., 1970. Variations in the pattern of pubertal changes in boys. Arch. Dis. Childhood 45, 13–23.
McIntosh, A.R., Mišić, B., 2013. Multivariate statistical analyses for neuroimaging data. Ann. Rev. Psychol. 64, 499–525.
McLaughlin, K.A., Colich, N.L., Rodman, A.M., Weissman, D.G., 2020. Mechanisms linking childhood trauma exposure and psychopathology: a transdiagnostic model of risk and resilience. BMC Med. 18, 96.
McIntosh, A.R., Lobaugh, N.J., 2004. Partial least squares analysis of neuroimaging data: applications and advances. NeuroImage 23 Suppl 1, S250–S263.
McLaughlin, K.A., Weissman, D., Bitrán, D., 2019. Childhood adversity and neural development: a systematic review. Ann. Rev. Dev. Psychol. 1, 277–312.
McLaughlin, K.A., Sheridan, M.A., 2016. Beyond Cumulative Risk: A Dimensional Approach to Childhood Adversity. Current directions in psychological science 25, 239–245.
McTeague, L.M., Huemer, J., Carreon, D.M., Jiang, Y., Eickhoff, S.B., Etkin, A., 2017. Identification of common neural circuit disruptions in cognitive control across Psychiatric disorders. Am. J. Psychiatry 174, 676–685.
Mennes, M., Zuo, X.N., Kelly, C., Di Martino, A., Zang, Y.F., Biswal, B., Castellanos, F.X., Milham, M.P., 2011. Linking inter-individual differences in neural activation and behavior to intrinsic brain dynamics. Neuroimage 54, 2950–2959.
Millán, A.P., Torres, J.J., Johnson, S., Marro, J., 2018. Concurrence of form and function in developing networks and its role in synaptic pruning. Nat. Commun. 9, 2236.
Millar, P.R., Ances, B.M., Gordon, B.A., Benzinger, T., Fagan, A.M., Morris, J.C., Balota, D.A., 2020a. Evaluating resting-state BOLD variability in relation to biomarkers of preclinical Alzheimer's disease. Neurobiol. Aging 96, 233–245.
Millar, P.R., Petersen, S.E., Ances, B.M., Gordon, B.A., Benzinger, T., Morris, J.C., Balota, D.A., 2020b. Evaluating the sensitivity of resting-state BOLD variability to age and cognition after controlling for motion and cardiovascular influences: a network-based approach. Cereb. Cortex 30, 5686–5701.
Miller, J.G., Ho, T.C., Humphreys, K.L., King, L.S., Foland-Ross, L.C., Colich, N.L., Ordaz, S.J., Lin, J., Gotlib, I.H., 2020. Early life stress, frontoamygdala connectivity, and biological aging in adolescence: a longitudinal investigation. Cereb. Cortex 30, 4269–4280.
Mills, K.L., Siegmund, K.D., Tamnes, C.K., Ferschmann, L., Wierenga, L.M., Bos, M., Luna, B., Li, C., Herting, M.M., 2021. Inter-individual variability in structural brain development from late childhood to young adulthood. NeuroImage 242, 118450.
Miočević, M., O'Rourke, H.P., MacKinnon, D.P., Brown, H.C., 2018. Statistical properties of four effect-size measures for mediation models. Behav. Res. Methods 50, 285–301.
Mirman, A., Bick, A.S., Kalla, C., Canetti, L., Segman, R., Dan, R., Ben Yehuda, A., Levin, N., Bonne, O., 2021. The imprint of childhood adversity on emotional processing in high functioning young adults. Hum. Brain Mapp. 42, 615–625.
Miskolczi, C., Halász, J., Mikics, É., 2019. Changes in neuroplasticity following early-life social adversities: the possible role of brain-derived neurotrophic factor. Pediatr. Res. 85, 225–233.
Modabbernia, A., Janiri, D., Doucet, G.E., Reichenberg, A., Frangou, S., 2021. Multivariate patterns of brain-behavior-environment associations in the adolescent brain and cognitive development study. Biol. Psychiatry 89, 510–520.
Moos, R.H., Moos, B.S., 1994. Family Environment Scale Manual. Consulting Psychologists Press, Palo Alto, CA.
Murray, E.A., Wise, S.P., Graham, K.S., 2017. The Evolution of Memory Systems: Ancestors, anatomy, and adaptations. Oxford University Press.
Murthy, S., Gould, E., 2020. How early life adversity influences defensive circuitry. Trends Neurosci. 43, 200–212.
Nelson 3rd, C.A., Gabard-Durnam, L.J., 2020. Early adversity and critical periods: neurodevelopmental consequences of violating the expectable environment. Trends Neurosci. 43, 133–143.
O'Craven, K.M., Kanwisher, N., 2000. Mental imagery of faces and places activates corresponding stimulus-specific brain regions. J. Cognit. Neurosci. 12, 1013–1023.
Owens, M.M., Allgaier, N., Hahn, S., Yuan, D.K., Albaugh, M., Adise, S., Chaarani, B., Ortigara, J., Juliano, A., Potter, A., Garavan, H., 2021. Multimethod investigation of the neurobiological basis of ADHD symptomatology in children aged 9-10: baseline data from the ABCD study. Trans. Psychiatry 11, 64.
Parade, S.H., Huffhines, L., Daniels, T.E., Stroud, L.R., Nugent, N.R., Tyrka, A.R., 2021. A systematic review of childhood maltreatment and DNA methylation: candidate gene and epigenome-wide approaches. Trans. Psychiatry 11, 134.
Park, B., Bethlehem, R., Paquola, C., Lariviere, S., Rodriguez-Cruces, R., Vos de Wael, R., NSPN, Bullmore, E., Bernhardt, B.C., 2021. An expanding manifold in transmodal regions characterizes adolescent reconfiguration of structural connectome organization. eLife 10, e64694.
Park, S., Chun, M.M., 2009. Different roles of the parahippocampal place area (PPA) and retrosplenial cortex (RSC) in panoramic scene perception. In: Neuroimage, 47, pp. 1747–1756.
Petersen, A.C., Crockett, L., Richards, M., Boxer, A., 1988. A self-report measure of pubertal status: reliability, validity, and initial norms. J. Youth Adolesc. 17, 117–133.
Peverill, M., Dirks, M.A., Narvaja, T., Herts, K.L., Comer, J.S., McLaughlin, K.A., 2021. Socioeconomic status and child psychopathology in the United States: a meta-analysis of population-based studies. Clin. Psychology Rev. 83, 101933.
Pfeifer, J.H., Allen, N.B., 2021. Puberty initiates cascading relationships between neurodevelopmental, social, and internalizing processes across adolescence. Biol. Psychiatry 2, 99–108.
Pierpaoli, C., Jezzard, P., Basser, P.J., Barnett, A., Di Chiro, G., 1996. Diffusion tensor MR imaging of the human brain. Radiology 201, 637–648.
Power, J.D., Schlaggar, B.L., Petersen, S.E., 2015. Recent progress and outstanding issues in motion correction in resting state fMRI. NeuroImage 105, 536–551.
Preacher, K.J., Kelley, K., 2011. Effect size measures for mediation models: quantitative strategies for communicating indirect effects. Psychol. Methods 16, 93–115.
Pur, D.R., Eagleson, R.A., de Ribaupierre, A., Mella, N., de Ribaupierre, S., 2019. Moderating effect of cortical thickness on BOLD signal variability age-related changes. Front. Aging Neurosci. 11, 46.
Quackenbush, J., 2002. Microarray data normalization and transformation. Nat. Genet. 32, 496–501.
Ramirez, J.S.B., Graham, A.M., Thompson, J.R., Zhu, J.Y., Sturgeon, D., Bagley, J.L., Thomas, E., Papadakis, S., Perrone, A., Earl, E., Miranda Dominguez, O., Feczko, E., Fombone, E.J., Amaral, D.G., Nigg, J.T., Sullivan, E.L., Fair, D., 2020. Maternal interleukin-6 is associated with macaque offspring amygdala development and behavior. Cereb. Cortex 30, 1573–1585.
Ramphal, B., DeSerisy, M., Pagliaccio, D., Raffanello, E., Rauh, V., Tau, G., Posner, J., Marsh, R., Margolis, A.E., 2020. Associations between amygdala-prefrontal functional connectivity and age depend on neighborhood socioeconomic status. . Cereb. Cortex Commun. 1, 033 tgaa033.
Rasmussen, J.M., Graham, A.M., Entringer, S., Gilmore, J.H., Styner, M., Fair, D.A., Wadhwa, P.D., Buss, C., 2019. Maternal Interleukin-6 concentration during pregnancy is associated with variation in frontolimbic white matter and cognitive development in early life. NeuroImage 185, 825–835.
Rosenberg, M.D., Martinez, S.A., Rapuano, K.M., Conley, M.I., Cohen, A.O., Corenjo, M. D., Hagler, D.J., Anderson, K.M., Wager, T.D., Feczko, E., Earl, E., Fair, D.A., Barch, D.M., Watts, R., Casey, B.J., 2020. Behavioral and neural signatures of working memory in childhood. J. Neurosci. 40, 5090–5104.
Satterthwaite, T.D., Wolf, D.H., Ruparel, K., Erus, G., Elliott, M.A., Eickhoff, S.B., Gennatas, E.D., Jackson, C., Prabhakaran, K., Smith, A., Hakonarson, H., Verma, R., Davatzikos, C., Gur, R.E., Gur, R.C., 2013. Heterogeneous impact of motion on fundamental patterns of developmental changes in functional connectivity during youth. NeuroImage 83, 45–57.
Schweizer, S., Satpute, A.B., Atzil, S., Field, A.P., Hitchcock, C., Black, M., Barrett, L.F., Dalgleish, T., 2019. The impact of affective information on working memory: A pair of meta-analytic reviews of behavioral and neuroimaging evidence. Psychol. Bull. 145, 566–609.
Selous, C., Kelly-Irving, M., Maughan, B., Eyre, O., Rice, F., Collishaw, S., 2020. Adverse childhood experiences and adult mood problems: evidence from a five-decade prospective birth cohort. Psychol. Med. 50, 2444–2451.
Simons, D.J., Shoda, Y., Lindsay, D.S., 2017. Constraints on Generality (COG): a proposed addition to all empirical papers. Perspect. Psychol. Sci. 12, 1123–1128.
Smith, S.M., Jenkinson, M., Woolrich, M.W., Beckmann, C.F., Behrens, T.E.J., Matthews, P.M., 2004. Advances in functional and structural MR image analysis and implementation as FSL. NeuroImage 23, 208–219.
Smith, S.M., Nichols, T.E., Vidaurre, D., Winkler, A.M., Behrens, T.E.J., Glasser, M.F., Miller, K.L., 2015. A positive-negative mode of population covariation links brain connectivity, demographics and behavior. Nat. Neurosci. 18, 1565–1567.
Snyder-Mackler, N., Burger, J.R., Gaydosh, L., Belsky, D.W., Noppert, G.A., Campos, F.A., Bartolomucci, A., Yang, Y.C., Aiello, A.E., O'Rand, A., Harris, K.M., Shively, C.A., Alberts, S.C., Tung, J., 2020. Social determinants of health and survival in humans and other animals. Science 368 eaax9553–14.
Stover, P.J., Harlan, W.R., Hammond, J.A., Hendershot, T., Hamilton, C.M., 2010. PhenX: a toolkit for interdisciplinary genetics research. Curr. Opin. Lipidol. 21, 136–140.
Sumner, J.A., Colich, N.L., Uddin, M., Armstrong, D., McLaughlin, K.A., 2019. Early experiences of threat, but not deprivation, are associated with accelerated biological aging in children and adolescents. Biol. Psychiatry 85, 268–278.
Sun, Y., Fang, J., Wan, Y., Su, P., Tao, F., 2020. Association of Early-Life Adversity With Measures of Accelerated Biological Aging Among Children in China. JAMA Netw. Open 3, e2013588.
Supek, F., Bošnjak, M., Škunca, N., Šmuc, T., 2011. REVIGO summarizes and visualizes long lists of Gene Ontology terms. PLoS One 6, 21800. https://doi.org/10.1371/journal.pone.0021800.
Suzuki, A., Poon, L., Kumari, V., Cleare, A.J., 2015. Fear biases in emotional face processing following childhood trauma as a marker of resilience and vulnerability to depression. Child Maltreat. 20, 240–250.
Thapar, A., Martin, J., Mick, E., Arias Vasquez, A., Langley, K., Scherer, S.W., Schacher, R., Crosbie, J., Williams, N., Franke, B., Elia, J., Glessner, J., Hakonarson, H., Owen, M.J., Faraone, S.V., O'Donovan, M.C., Holmans, P., 2016. Psychiatric gene discoveries shape evidence on ADHD's biology. Mol. Psychiatry 21, 1202–1207.
Thijssen, S., Collins, P., Luciana, M., 2020. Pubertal development mediates the association between family environment and brain structure and function in childhood. Dev. Psychopathol. 32, 687–702.
Thompson, A., Schel, M.A., Steinbeis, N., 2021. Changes in BOLD variability are linked to the development of variable response inhibition. NeuroImage 228, 117691.

Tofighi, D., Kelley, K., 2020. Indirect effects in sequential mediation models: Evaluating methods for hypothesis testing and confidence interval formation. Mult. Behav. Res. 55, 188–210.
Tooley, U.A., Bassett, D.S., Mackey, A.P., 2021. Environmental influences on the pace of brain development. Nat. Rev. Neurosci. 22, 372–384.
Tooley, U.A., Mackey, A.P., Ciric, R., Ruparel, K., Moore, T.M., Gur, R.C., Gur, R.E., Satterthwaite, T.D., Bassett, D.S., 2020. Associations between neighborhood SES and functional brain network development. Cereb. Cortex 30, 1–19.
Tottenham, N., Tanaka, J., Leon, A.C., McCarry, T., Nurse, M., Hare, T.A., Marcus, D.J., Westerlund, A., Casey, B.J., Nelson, C.A., 2009. The NimStim set of facial expressions: judgments from untrained research participants. Psychiatry Res. 168, 242–249.
Tozzi, L., Staveland, B., Holt-Gosselin, B., Chesnut, M., Chang, S.E., Choi, D., Shiner, M. L., Wu, H., Lerma-Usabiaga, G., Sporns, O., Barch, D., Gotlib, I.H., Hastie, T.J., Kerr, A.B., Poldrack, R.A., Wandell, B.A., Wintermark, M., Williams, L.M., 2020. The human connectome project for disordered emotional states: Protocol and rationale for a research domain criteria study of brain connectivity in young adult anxiety and depression. NeuroImage 124, 116715.
Tsvetanov, K.A., Henson, R.N.A., Tyler, L.K., Razi, A., Geerligs, L., Ham, T.E., Rowe, J.B., 2016. Extrinsic and intrinsic brain network connectivity maintains cognition across the lifespan despite accelerated decay of regional brain activation. J. Neurosci. 36, 3115–3126.
Tyborowska, A., Volman, I., Niermann, H., Pouwels, J.L., Smeekens, S., Cillessen, A., Toni, I., Roelofs, K., 2018. Early-life and pubertal stress differentially modulate grey matter development in human adolescents. Sci. Rep. 8, 9201. https://doi.org/10.1038/s41598-018-27439-5.
Vakorin, V.A., Lippe, S., McIntosh, A.R., 2011. Variability of brain signals processed locally transforms into higher connectivity with brain development. J. Neurosci. 31, 6405–6413.
Vargas, T., Damme, K.S.F., Mittal, V.A., 2020. Neighborhood deprivation, prefrontal morphology and neurocognition in late childhood to early adolescence. NeuroImage 220, 117086.
Vatansever, D., Bzdok, D., Wang, H., Mollo, G., Sormaz, M., Murphy, C., Jefferies, E., 2017. Varieties of semantic cognition revealed through simultaneous decomposition of intrinsic brain connectivity and behaviour. NeuroImage 158, 1–11.
Vettel, J.M., Cooper, N., Garcia, Javier, O., Yeh, F.-C., Verstynen, T.D., 2017. White matter tractography and diffusion-weighted Imaging. eLS. John Wiley & Sons, Ltd, Chichester.
Vogel, S.C., Perry, R.E., Brandes-Aitken, A., Braren, S., Blair, C., 2021. Deprivation and threat as developmental mediators in the relation between early life socioeconomic status and executive functioning outcomes in early childhood. Dev. Cognit. Neurosci. 47, 100907.
Walters, G.D., 2018. PM effect size estimation for mediation analysis: a cautionary note, alternate strategy, and real data illustration. Int. J. Social Res. Methodol. 21, 25–33.
Wang, H., Ghaderi, A., Long, X., Reynolds, J.E., Lebel, C., Protzner, A.B., 2021. The longitudinal relationship between BOLD signal variability changes and white matter maturation during early childhood. NeuroImage 242, 118448.
Wang, H.-T., Smallwood, J., Mourao-Miranda, J., Xia, C.H., Satterthwaite, T.D., Bassett, D.S., Bzdok, D., 2020. Finding the needle in a high-dimensional haystack: Canonical correlation analysis for neuroscientists. NeuroImage 216, 116745.
Waschke, L., Kloosterman, N., Obleser, J., Garrett, D.D., 2021. Behaviour needs neural variability. Neuron 109, 1–16.
Wells 3rd, W.M., Viola, P., Atsumi, H., Nakajima, S., Kikinis, R., 1996. Multi-modal volume registration by maximization of mutual information. Med. Image Anal. 1, 35–51.
Whitaker, K.J., Vértes, P.E., Romero-Garcia, R., Váša, F., Moutoussis, M., Prabhu, G., Bullmore, E.T., 2016. Adolescence is associated with genomically patterned consolidation of the hubs of the human brain connectome. Proc. Natl. Acad. Sci. U. S. A. 113, 9105–9110.
Wig, G.S., Schlaggar, B.L., Petersen, S.E., 2011. Concepts and principles in the analysis of brain networks. Ann. N. Y. Acad. Sci. 1224, 126–146.
Worthman, C.M., Trang, K., 2018. Dynamics of body time, social time and life history at adolescence. Nature 554, 451–457.
Zhuang, J., Hrabe, J., Kangarlu, A., Xu, D., Bansal, R., Branch, C.A., Peterson, B.S., 2006. Correction of eddy-current distortions in diffusion tensor images using the known directions and strengths of diffusion gradients. J. Magn. Resonance Imag. 24, 1188–1193.
Zou, Q., Ross, T.J., Gu, H., Geng, X., Zuo, X.N., Hong, L.E., Gao, J.H., Stein, E.A., Zang, Y. F., Yang, Y., 2013. Intrinsic resting-state activity predicts working memory brain activation and behavioral performance. Hum. Brain Mapp. 34, 3204–3215.
Zucker, R.A., Gonzalez, R., Feldstein Ewing, S.W., Paulus, M.P., Arroyo, J., Fuligni, A., Morris, A.S., Sanchez, M., Wills, T., 2018. Assessment of culture and environment in the Adolescent Brain and Cognitive Development Study: Rationale, description of measures, and early data. Dev. Cognit. Neurosci. 32, 107–120.